5-1-2013

The Effects of Glutathione and Its Derivatives on the Survival of Mycobacterium bovis-BCG Vegetative and Persistent Organisms

Neil Patel
Honors College, Pace Univesity

Title: The Effects of Glutathione and Its Derivatives on the Survival of *Mycobacterium bovis*-BCG Vegetative and Persistent Organisms

Type of manuscript: Article

Author: Neil D. Patel

Keywords: Glutathione, Mycothiol, HPLC, NRP, Mycobacterium, *M. tuberculosis*, *M. bovis* – BCG

Abstract

Mycobacterium tuberculosis is responsible for nearly 2 million deaths yearly. Upon inhalation, mycobacteria are engulfed by alveolar macrophages. These cells produce reactive oxygen and nitrogen intermediates (ROI's and RNI's), which normally kill pathogens, but are ineffective against invading mycobacteria. What ensues, is the formation of a tubercle to sequester the infected macrophages, and the initiation of a latent tuberculosis infection, in which the mycobacteria enter a state of non-replicative persistence (NRP). Glutathione (GSH), a host tripeptide thiol-based detoxification molecule, protects host cells from ROI/RNI toxicity. Recently, it has been demonstrated that GSH is toxic to *in vitro* and early infection mycobacteria, but no studies determined whether GSH is toxic to latent mycobacteria. To further elucidate the impact of GSH on mycobacteria, we exposed mid-logarithmic (mid-log) and NRP-induced *M. bovis*-BCG to glutathione in its reduced (GSH), oxidized (GSSG), and nitric oxide associated (GSNO) forms, for five days. We have demonstrated that the growth of mid-log *M. bovis-BCG* (BCG) is inhibited by 4 mM GSH, and killed by 8 mM GSH. The growth of NRP mycobacteria exposed to 4 mM GSH was inhibited similar to that of unexposed NRP mycobacteria. In contrast, the growth of NRP BCG is stimulated four fold following exposure to 8 mM GSH. We conclude that exposure of NRP BCG to 8 mM GSH stimulates exit from the NRP state into an actively metabolizing state. 4 and 8 mM GSSG and GSNO inhibited the growth of mid-log BCG; however, NRP BCG exposed to GSSG and GSNO inhibited growth similar to that of unexposed NRP BCG. These results were confirmed by performing viability studies, and analysis of free-intracellular cytoplasmic ATP concentrations. Initially hypothesized, the toxicity to GSH was due to redox potential imbalances within mycobacterial cytoplasm. Mycobacteria contain MSH detoxification system (5), to cope with GSH. However, the mechanism of interaction between the activation of the system and growth inhibition in mycobacteria is poorly understood. HPLC analyses on mid-log and NRP BCG cytoplasms exposed to 4 and 8 mM GSH demonstrated that the activation of the detoxification system and the oxidative stress of the mid-log and NRP cytoplasms were similar. This suggests that the activation of the detoxification system and the oxidative state of the mycobacterial cytoplasm may not play a direct role in mycobacterial growth inhibition and/or exit from the NRP state.

Introduction

Currently, one third of the world's population is infected by Mycobacterium *tuberculosis*, the causative agent of tuberculosis. The organism is responsible for nearly 2 million deaths per year. Although these ratios are not predominant in the United States, underdeveloped countries primarily contribute the increase in the number of deaths per year. This is attributed to the lack of antibiotics accessibility to antibiotics, as well as the rise of antibiotic resistant strains. In relation to the infection, a small percent of the infected population is able to clear the infection and be asymptomatic. Majority of patients infected with tuberculosis are either in active or latent infection.

Innate Immune Response

Upon inhalation of *M. tuberculosis* aerosols from an infected individual, the primary site of infection resides within the inner lining of the lungs. Present resident alveolar macrophages engulf the bacilli and isolate them within the phagosome. Within the phagosome, reactive nitrogen intermediate (RNI) and reactive oxygen intermediates (ROI) are introduced to the bacteria, creating a toxic environment aimed to kill the pathogen (2). These intermediates are used to perturb the oxidative balance of the invading microorganism, leading to cell death. Additional defense abilities of the macrophage include acidification of the phagosome, and phagosome fusion with the lysosome (37). These acidification processes, are aimed to destroy internal structures and proteins of the bacteria, leading to cell death. *M. tuberculosis* is able to evade this innate immune response by initiating factors that inhibit acidification by preventing phagolysosomal fusion (1). In addition, they are able to overcome the oxidative stress introduced by the host by using catalase/peroxidase enzyme (KatG) (23), superoxide dismutase (43), and a thiol-based detoxification system (36). Collectively, these factors assist the bacteria to evade multiple components of the host immune response, allowing them to persist, and replicate within the macrophage.

Bacilli that are able to elude the adverse oxidative effects and phagosomal acidification processes continue to multiply logarithmically for approximately two weeks after initial infection inside the macrophage. At this point macrophages release chemokines and interferon-γ (IFNγ) to actuate T-cell immunity and antigen-specific T lymphocytes, which further activate the macrophages to kill the bacteria. However, this specific cell mediated immune response is unable to eliminate the pathogen from the host, leading to the formation of a granulomatous region called a tubercle; initiating latent infection (37). Chemokines and cytokines are produced by infiltrating leukocytes and local tissue to maintain the formation of the tubercle (35). The infiltration of these intermediates, at increased concentrations, creates a central region of necrotic tissue within the granuloma; the mycobacteria in turn use this necrotic tissue for nutrients (35). In the core of the granuloma, the reactive nitrogen, oxygen, and other toxic immune components create an hypoxic environment which leads to the formation of necrotic tissue. The coupling of these two mechanisms limits the metabolic capabilities of the bacteria, in addition to limiting the amount of available nutrients for the bacteria, over time. As a result, there are changes in gene expression that force the bacteria into latent Tb infection (LTBI) (30).

Studies performed my Wayne *et al.* (2001) show that the transition to latent infection occurs in successive stages, which are O_2 dependent. The gradual depletion of oxygen leads to nonreplicative persistence (NRP) state that is characterized by bacteriostasis, metabolic, chromosomal, and structural changes in quiescent bacteria. In addition, the NRP state is characterized by a shift from rapid to slow growth, significantly reduced metabolic activity, followed by a complete shutdown of cell cycle progression (12). An adaptive process associated with the NRP state in *M. tuberculosis* is the *Dos*-response (*Dos*R). Activation of this response allows the bacteria to enter the NRP state in order to withstand extended alternative growth conditions, such as those present in the host (12).

DosT/S/R

In order to stimulate the latent NRP state *in vivo* in murine models, the bacteria require the factors interferon- γ, tumor necrosis factor, or nitric oxide (4). When initiating latency *in vitro*, the dormant state can be established by nutrient deprivation (4) and oxygen depletion (40). In addition, low, non-toxic concentrations of NO are able to induce dormancy in mycobacteria (38). Specifically, the NO competes with O_2 to bind to DosR, inducing 48 latency genes. The DosR regulon is expressed when exposed to nontoxic concentrations of NO and CO, and the induction of the regulon is inhibited in the presence of oxygen (3, 19, 20, 28, 29, 31, 32, 34, 38, 42). Two important signal regulators DosT and DosS autophosphorylate, then transfer a phosphate to the DosR regulon, activating DosR (27). Both the DosT and DosS sensors are bound to heme groups that bind to the activating or deactivating divalent gasses: NO, CO, and O_2. The interactions of the divalents with the heme group are responsible for ultimately activating and deactivating DosR (6, 19, 28, 29, 33). DosT is identified to be the hypoxia sensor; when oxygen is bound to DosT the activation of DosR is inhibited. When the heme group present on the DosS receptor is oxidized in the presence of high oxygen concentrations, DosR sensor is rendered inactive. DosS however is the redox sensor, once the heme group on the sensor is reduced to Fe^{2+} from Fe^{3+}, signaling for DosR activation occurs (6, 19). It is possible for NO and CO to displace O2 from the DosS and DosT heme groups, resulting in activation of DosR (6, 21). Due to the high binding affinities of NO and CO to the iron present in the heme group, they are capable of locking the DosR sensor in the active state. Overall, the induction and maintenance of NRP due to DosR activation is dependent on the presence and concentration of CO and NO

Glutathione

Simultaneous to the production of ROIs and RNIs, the cells of the immune response produce glutathione (GSH), a component of the host thiol-based detoxification system. GSH is a tripeptide comprised of γ-glutamate, cysteine, and glycine, which functions as an antioxidant found in all cells of the body, including macrophages (9). Glutathione protects phagocytic host cells from oxidative toxicity associated with the release of ROIs and RNIs, chemokines, and cytokines, by maintaining a reduced environment within the host cytoplasms (36). The intracellular host concentration of GSH is approximately 1-8 mM, and is 1000 fold higher than the plasma concentration, which is approximately 5-50 μM (11, 16). During oxidative stress, GSH is oxidized to glutathione thiodisulphide (GSSG); GSSG is converted back to GSH by GSH reductase; a NADPH-cofactor requiring conversion (11, 16). In contrast to GSH, GSSG acts to maintain a reduced

environment for in organellic structures within the host macrophage. In addition, GSH can react with NO to form *S*-nitrosoglutathione (GSNO); the stability of NO is increased once bound with GSH (9). During initial infection, GSNO serves as an NO donor to interfere with the pathogenesis of invading microorganisms including mycobacteria (10, 25). GSNO has been shown to be responsible for killing *M. tuberculosis* in mice (15).

GSH can be transported into the bacterial cell as a tripeptide, dipeptide, or single amino acids using ABC oligopeptide transporters (Opp) (7). Exoenzymes secreted by *Mtb* are able to break down GSH into it a dipeptide, and into its individual amino acids. The action of the exoenzyme γ-glutamyl transpeptidase (GgtA), GSH is cleaved into cys-gly and γ-glutamate (10, 22). Cys-Gly is transported into the cell by an ABC transporter dipeptide permease (Dpp) (9). Although in-depth analyses have been performed, the mechanism of GSH toxicity in mycobacteria is still unknown. A prevalent theory suggests that an imbalance is created in the mycobacterial thiol detoxification system (mycothiol), leading to an oxidation/reduction imbalance, resulting in cell death (26). This imbalance is created due to the import of cys-gly into the mycobacteria cell (9).

Bacterial Mycothiol (MSH)

Bacterial mycothiol (MSH) is the major low-molecular-mass thiol present in mycobacteria. MSH is found only in actinomycetes, and at high concentrations in *Mycobacterium tuberculosis*. The functionality of mycothiol is analogous to that of mammalian thiol based detoxification system – glutathione. It is known that glutathione is not present in *Mtb*. Therefore, similar to glutathione; mycothiol acts to maintain the oxidative state of the mycobacterial cell; by interconverting between MSH and MSSM. Mycothiol activity protects *M. tuberculosis* from toxic oxidants produced by antibiotics and the macrophage itself, such as ROIs and RNIs (5). An alteration in mycothiol activity is shown to alter the overall oxidation state of the bacterial cell. Specifically, an altered oxidation state can influence the cell wall components altering the cell wall permeability, leading to greater molecule exchange between extracellular and intracellular components and bacterial cell death (5). By evaluating the oxidative balance of mycothiol upon exposure to toxic concentrations of glutathione will help elucidate the function of glutathione.

Primary Focus

It has recently been demonstrated that both GSH and GSNO are toxic to mycobacteria both *in vitro* and *in vivo* early infection models (prior to the formation of the tubercle) (9). GSNO toxicity is likely due to the mycobactericidal effects of NO release from GSNO (7). It has been hypothesized that the toxicity to GSH results from a redox potential imbalance in the mycobacterial cytoplasm leading to growth inhibition. *In vitro* studies have demonstrated that *M. tuberculosis* uses MSH to cope with both GSH and GSNO (2) but, the underlying mechanisms surrounding the balance between the activation of this system and mycobacterial killing *in vitro* and *in vivo* early infection models is poorly understood. In addition, there have been no studies to determine if GSH and GSNO are toxic to mycobacteria residing within the tubercle during latent infection. In order to further confirm previous studies and continue investigation of *M. tuberculosis* in the NRP state, both mid-logarithmic and NRP cells were treated with GSH, GSSG, and

GSNO, over five days, at concentrations of 4 mM and 8 mM concentrations; these concentrations mimic GSH levels present within the alveolar macrophage. We performed growth studies supplemented with the cell viability assays, and intracellular free ATP concentration assays to determine the bacteriostatic and bactericidal effects of each glutathione derivative at the varying concentrations. HPLC analysis was performed to investigate the impact of glutathione on the oxidative state of the mycobacterial cytoplasm.

We confirmed that 4 mM GSH is bacteriostatic, and 8 mM GSH is bactericidal to mid-log *M. bovis*-BCG over five days. In addition, our results showed that 4 mM and 8 mM GSSG and GSNO were bacteriostatic to mid-log *M. bovis*-BCG over the five-day period. NRP BCG exposed to 4 mM GSH, and 4 mM and 8 mM GSSG and GSNO showed no significant impact on the growth of NRP BCG. Surprisingly, 8 mM GSH with NRP BCG showed an increase in growth, suggesting exit from the NRP state. HPLC analysis confirms that stimulated growth is not due to an imbalance in the oxidative state of the mycobacterial cytoplasm. Our new hypothesis suggests that the transition from NRP to mid-log is due to cellular signaling, resulting in a deactivation of the DosR system due to the binding of oxygen to the DosT receptor.

Material and Methods

Bacterial Strains and Growth

M. bovis-BCG Pasteur strain was grown in Middlebrook medium. Middlebrook 7H9 (liquid) and 7H11 (1.5% agar) media (Sigma) were supplemented with glycerol (0.5%, vol/vol) and ADC supplement (0.5% albumin – from bovine serum [Sigma], 0.2% dextrose, 0.85% NaCl). All liquid cultures of BCG were supplemented with 0.05% Tween 80 (Sigma). All cultures were incubated in a rotating incubator at 37°C

Mid-log BCG cells were inoculated in in 7H9 supplemented with glycerol (0.5%, vol/vol) and ADC supplement (0.5% albumin – from bovine serum [Sigma], 0.2% dextrose, 0.85% NaCl). The non-replicating persistence (NRP) oxygen depletion model developed by Hu and colleagues (2003) was replicated to induce NRP BCG (*in vitro*) cells at 37°C. NRP cells remained stationary for 100 days, without agitation, in a low oxygen environment.

M. bovis – BCG Growth Curve

Five-day growth cultures were inoculated on day 1 with mid-logarithmic BCG or NRP BCG at OD_{600} of 0.1, in 7H9 media with ampicillin (1 mg/mL) in 15 mL sterile conical tubes. 1 mL aliquots were removed daily to assess cell density at OD_{600} over five days. All mid-log BCG cultures were incubated in a shaking incubator. All liquid NRP trail cultures were placed in a stand still incubator. Sterile glass beads were added to each NRP trail tube to compensate for the volume displacement to ensure an anoxic environment. All samples were incubated at 37°C.

Trails consisted of samples at 0 mM, 4 mM, and 8 mM concentrations of GSH, GSSG, and GSNO. 4 mM and 8 mM GSH and GSSG were added daily for four days. Samples treated with GSNO were inoculated at concentrations of 4 mM, and 8 mM only once, on the initial day. Each trail was performed in triplicate.

M. bovis –BCG Inhibition/Killing Viability Assay

A 10 µL aliquot of each sample was removed while performing the growth curve studies, and were diluted by a (1/100,000 serial dilution), and 100 µL were plated on 7H11 agar. Plates were incubated at 37°C for 27 days. CFU were quantitated and normalized according to the dilution factor.

M. bovis –BCG Cell Intracellular ATP Quantization

Quantitation of intracellular ATP was performed according to the *BacTiter-Glo™ Microbial Cell Viability Assay [Promega]*. Samples were removed daily and diluted to OD_{600} of 0.1. The chemiluminescence of the ATP reaction was determined using a Gel Logic 2200 PRO luminometer.

Cell Extraction for Thiols Analysis

Cell aliquots were taken in triplicates from the growth trails and normalized to OD_{600} of 0.1. Extracts were labeled with monobromobimine (mBBr) for thiol analysis as described in Newton *et al.* (1996). Modifications were made in which cell extracts were micro-centrifuged at 3,000xg, 10 min, 4 ^{0}C; aspiration of the media was performed, and cells were resuspended in 0.500 mL inactivation buffer [20 mM HEPES buffer (pH 8.0), 50% ACN, and 2 mM mBBr]. Cells were

placed at 60 ^{0}C for 15 min, and were micro-centrifuged at 21,100xg for 20 min; to pellet cellular debris. Supernatants was aspirated, and stored at -80 ^{0}C.

HPLC Analyses of Thiol-mB Derivatives

The thiol bimine derivatives (RSmB) were analyzed using a modified HPLC method 1 (13, 24) to provide improved separation of the compounds. A LC 410 pump (Perkin-Elmer, Norwalk, CT) coupled to a C-18 10um column (4.5mm x 250mm) at a flow rate of 1 ml min^{-1} was used with buffers A (0.25% acetic acid in H2O titrated to pH 3.6 with NaOH) and buffer B (HPLC grade methanol, Fisher). The linear gradient was as follows: 0 min, 10% B; 10 min, 10% B; 25 min, 18% B; 40 min, 27% B; 50 min, 50% B; 60 min, 100% B; 65 min, 10% B; 75 min, 10% B reinject. The retention times are as follows: 2:16 min, γ-glu-cys; 12:12 min, L-cys; 10:48 min, cys-gly; 12:12 min, GSH; 18:32 min, MSH. NRP Samples were diluted 1:1 using methanesulfonic acid prior to injection.

Results

M. bovis – BCG GSH Growth Curve

In order to investigate the effect of glutathione on the growth of BCG, we performed triplicate growth trials over five days by exposing BCG to 4 and 8 mM GSH. On Day 1, unexposed, 4 mM, and 8 mM mid- log and NRP samples were all normalized to an OD_{600} of 0.1 (Figure 1a). Spectrophotometer analyses of bacterial growth over five days upon exposure to GSH shows that mid-logarithmic unexposed BCG exponentially grew to reach a maximum OD_{600} of 0.797 on Day 4. Mid-logarithmic BCG exposed to 8 mM GSH show decreased levels in bacterial growth – reaching a maximum OD_{600} of 0.240. Mid-logarithmic BCG exposed to 4 mM GSH over five days resulted in similar optical densities to that of unexposed BCG; having a maximum OD_{600} of 0.694. These growth studies propose that GSH is toxic to mid-log BCG over five days. However, they do not confirm if the cells are being inhibited or killed.

Optical density analyses performed on NRP BCG (Figure 1b) resulted in no significant increase in growth of unexposed NRP bacteria. The maximum OD_{600} reached was 0.131. Similar results are shown for NRP BCG exposed to 4 mM GSH over a five-day period. The maximum OD_{600} was 0.135. NRP BCG exposed for 8 mM GSH over five days, resulted in a significant increase in optical density. On Days 1, 2, and 3 the highest OD_{600} of 8 mM NRP BCG was 0.125. Remarkably, on Day 4 the OD_{600} increased to 0.207, and on Day 5 the OD_{600} of 8 mM NRP BCG was 0.398. These results suggest that 8 mM GSH facilitates in the exit from the NRP state to mid-logarithmic growth.

M. bovis –BCG GSH Inhibition/Killing Viability Assay

Based off the results obtained from the growth studies, in order to determine whether GSH inhibited or killed mid-log and NRP BCG, we performed cell viability assays. On Day 1, unexposed, 4 mM, and 8 mM mid- log and NRP samples were all normalized to a bacterial count of 1.0×10^8 bacterial cells per mL. The mid-log (Figure 2a) unexposed results show that there is an average of 2.5×10^9 total viable cells over five days. Mid-log BCG exposed to 4 mM GSH, show there are viable bacterial cells, with a total average cell count of 2.2×10^9 over the five-day period. In contrast, mid-log BCG exposed to 8 mM GSH exhibited no colony forming units on Day 4 and 5. Viable CFU were quantitated between Day 1 and 3 for mid-log 8 mM GSH exposed BCG. On Day 3, mid-log BCG exposed to 8 mM GSH presented an average cell count of 3.0×10^9; similar to that of 0 and 4 mM GSH exposed mid-log BCG. The cell viability of 8 mM GSH exposed mid-log BCG was conducted to investigate the number of viable cells in relation to the growth curve pattern. These killing results show to be consistent with the growth curve pattern. They confirm that the bacterial cells are indeed being killed over five days.

NRP BCG (Figure 2b) exposed to 4 and 8 mM GSH did not show statistically significant deviations in cell count on days 1, 2, 3, and 4. Viability analysis of NRP BCG on Day 5 shows an increase in the number of bacterial cells for unexposed, 4 mM GSH, and 8 mM GSH. Normalization of the data presented in Figure 2c to an OD_{600} of 0.1 shows on Day 5 there are less viable bacterial cells upon exposure to 8 mM GSH. On Day 5 of the NRP BCG viability trials, there were 3.53×10^8 viable unexposed BCG cells; 3.34×10^8 viable 4 mM exposed BCG cells, and 9.59×10^7 viable 8 mM exposed BCG cells. The lower viability noted after normalization

indicates that BCG is exiting the NRP state to mid-log growth. During this transition, GSH then kills the BCG, as seen in the mid-log growth trials.

M. bovis – BCG GSH Exposed Intracellular ATP Quantization

The ATP assays were performed to determine the free ATP present in mid-log cells in comparison to NRP to confirm that the NRP state maintains a low metabolic profile, consistent with low metabolic energetic needs. Also, by evaluating the free intracellular ATP concentrations present within the cells over the five days upon exposure to GSH, we were able to confirm the killing of mid-log and NRP BCG. In addition, evaluating the energetics of the cell helped elucidate the cellular response upon exposure to glutathione. Normalization of mid-log BCG cells (Figure 3a) on Day 1 resulted in an intracellular ATP concentration of 0.108 uM (unexposed BCG), 0.117 uM (4 mM GSH exposed), and 0.130 uM – (8 mM GSH exposed). On Day 5, unexposed mid-log BCG intracellular ATP concentration reached a maximum of 1.380 uM. However, over the 5 day period, the ATP concentration was between 0.108 – 1.380 uM. The ATP concentration within 8 mM GSH exposed mid-log BCG was between 0.130 – 2.284 uM. On Day 3, the ATP concentration of 8 mM GSH mid-log BCG was 1.596 uM; on Day 4 the concentration increased to 2.284 uM, and on Day 5, the 8 mM GSH mid-log ATP concentration decreased to 0.779 uM. These results suggest that through Day 3 there is an increase in ATP in samples treated with 8 mM GSH, in attempts to overcome the toxicity of glutathione. On days 4 and 5 a decrease in free intracellular ATP is noted due to cell death; confirmed by the cell viability assay. This 17.5 fold increase in intracellular free ATP can be explained through two perspectives. The first relies on the basis of activation of the bacterial SOS response, in which the cell increases its metabolic needs, DNA repair mechanisms, increased protein output, and increased cellular respiration in order to overcome the external stress.

For NRP BCG the assay helped determine whether the energetic needs of the cell were increased or decreased to facilitate the exit from the NRP state. Intracellular ATP concentration in NRP BCG (Figure 3b) was minimal in 8 mM GSH in days 1-5, while unexposed BCG showed increased concentrations on day 3, 4, and 5. The initial Day 1 ATP concentration for unexposed NRP BCG was 0.017 uM. The following days showed increased levels between 0.746 – 1.698 uM between days three and five. NRP BCG exposed to 8 mM GSH showed on Day 1, 2, 3, and 4 to have intracellular ATP concentrations between 0.016 – 0.045 uM. On Day 3, an increase in intracellular ATP is noted at 0.197 uM; the maximum over the five day trial. The lack of increase in ATP over the five days is suggestive that an upregulation in ATP production is not seen because the ATP is being utilized to exit the NRP state.

M. bovis – BCG GSH Exposed HPLC Thiol Analysis

In order to further investigate the role of GSH with respect to the oxidative state of the mycobacterial cytoplasm, we performed thiol HPLC analysis on mid-log and NRP BCG over five days. This analysis was used to compare the intracellular levels of GSH, MSH, Cys-Gly, L-cys, and γ-glutamate. Alterations in these various compounds will elucidate oxidative changes that occur due to the direct or indirect interaction of GSH in NRP BCG. Figures 4 a, b, and c, show the separation of exposed NRP BCG intracellular compounds based on the Thiol analysis as described above. This separation was performed using 0.25% Acetic Acid (pH 4.2) for increased separation between cys-gly/L-cys (12;36 min), mixture of GSH, and/or dipeptide cys-Gly and/or L-cys (14:55 min) and MSH (18:52 min). Due to the relative similarities of GSH,

cys-gly, and L-cys, complete separation of the peaks for cys-gly, L-cys, and GSH is not shown. These results show an increase in base area for cys-gly and L-cys in samples exposed to 8 mM GSH (Figure 4a/c). There is an increase in either GSH/cys-gly/L-cys, which over five days gives raise to the mixture-defined region. This base widening is noted on Day 5 in all triplicate samples of 8 mM GSH NRP BCG. In comparison to unexposed NRP BCG samples (Figure 4a/b), there is no significant expansion of the mixture-defined region over five days. Which suggest that there is no import of GSH, cys-gly, or L-cys into the mycobacterial cell. With respect to mycothiol (Figure 4d) the average base area correlating to the concentration of MSH in 1 x 10^8 bacterial cells is not significantly different over the five days when comparing unexposed and 8 mM GSH exposed cells. The average base area concentration seen between days 1 and 3 is 11,000 – 13,000 units. On Day 4 however, a decrease in mycothiol concentration is noted in 8 mM GSH exposed samples. In comparison to the data as a whole, there is no significant difference in the mycothiol concentration data represented for both exposed and 8 mM GSH exposed NRP BCG. These results confirm that there is no significant change in the oxidative balance of the mycobacterial cell. However, in NRP BCG exposed to 8 mM GSH, the decrease in mycothiol on Day 4 may be attributed to the exit from the NRP state due to GSH and oxygen.

M. bovis – BCG GSSG Growth Curve

Similar to the growth curve of GSH, in order to investigate the effect of oxidized glutathione on the growth of BCG, we performed growth triplicate growth trials over five days by exposing BCG to 4 and 8 mM GSSG. On Day 1, all culture presented were normalized to an OD_{600} of 0.1. Mid-log BCG exposed to the oxidized glutathione, GSSG (Figure 5a), at concentrations of 4 and 8 mM shows results similar to that of mid-log BCG exposed to GSH. Unexposed BCG followed the exponential mid-logarithmic growth patter, and over the five days increased to an OD_{600} of 0.773. Mid-log BCG exposed to 4 mM GSSG, showed limited growth between Days 2-5. An OD_{600} of 0.258 – 0.314 was maintained over that four day period. 8 mM GSSG exposed mid-log BCG showed an increase to OD_{600} of 0.238 on Day 2; and decreased to OD_{600} of 0.120 on Day 5. These results suggest that GSSG is toxic to mid-log BCG, however these studies do not confirm cell death or inhibition. To further confirm the toxicity of GSSG, plating assays were performed.

On Day 1, all NRP samples were normalized to an OD_{600} of 0.1. NRP BCG exposed to GSSG (Figure 5b) showed no statistical deviations when exposed to 4 and 8 mM GSSG compared to unexposed BCG over five days. Between Day 2-5, the cell density increased to an average OD_{600} of 0.249, for unexposed, 4 mM GSSG, and 8 mM GSSG. These growth results suggest that GSSG has no effect on the growth of NRP BCG over five days; to validate these results, plating assays were performed.

M. bovis –BCG GSSG Inhibition/Killing Viability Assay

After performing growth studies to evaluate the effects of GSSG on mid-log and NRP BCG, we performed cell plating assays to determine whether GSSG inhibited or killed the BCG. The cell viability assay for mid-log BCG exposed to GSSG (Figure 6a) shows an increase in the number of viable unexposed bacterial cells present over the five days. Over the five-day trial period, there was a maximum of 4.74 x 10^9 viable unexposed mid-log BCG cells present on Day 4. Mid-log BCG treated with 4 mM GSSG showed in increase in viable cell count throughout the five days, increasing to 5.44 x 10^9 cells on Day 5. In addition, mid-log BCG exposed to 8 mM GSSG

showed an increase in viable cell count over the five-day period. The maximum number of viable cells is noted on Day 5 to 4.09 x 10^9 cells. Analysis of these results confirms that both 4 mM and 8 mM GSSG is capable of inhibiting mid-log BCG, but are unable to kill the bacteria.

NRP BCG cells treated with 4 mM and 8 mM GSSG (Figure 6b) showed a viable number of cells over five days. In comparison to unexposed NRP BCG cells, which also showed a viable number of cells over five days is comparable to that of GSSG treated cells. Over the five days, all three trial types had an average of approximately 2 x 10^7 viable cells. No significant deviation or change is noted in the number of quantifiable bacterial cells in each trial. These results confirm that upon exposure to varying concentrations of GSSG, the growth and viability of NRP BCG is not affected.

Mid-log and NRP BCG GSSG Exposed Intracellular ATP Quantization

After confirming the inhibition of mid-log BCG growth upon exposure to GSSG, we performed intracellular ATP assays to determine the utilization and accumulation of ATP in the cells over five days. Intracellular ATP analysis of mid-log BCG exposed to 4 and 8 mM GSSG (Figure 7a) show to have similar trends in intracellular ATP concentrations over five days; consistent with that of unexposed mid-log BCG. On Day 1, the average intracellular concentration of unexposed, 4 mM GSSG exposed, and 8 mM GSSG exposed was 0.091 uM. Unexposed mid-log BCG presented an average intracellular ATP concentration of 1.308 uM on Day 4, and 1.149 uM on Day 5. 4 mM GSSG exposed mid-log BCG presented increased intracellular ATP concentrations on Day 2 (0.336 uM), Day 3 (1.029 uM), and Day 4 (1.773 uM). A decrease to 1.294 uM was noted on Day 5 in comparison to Day 4. When mid-log BCG is treated with 8 mM GSSG, an increase in intracellular ATP is presented through Day 4. Similar to that of 4 mM GSSG, a significant decrease in intracellular ATP concentrations is noted. Between Day 1 and 4, the intracellular ATP concentration increases from 0.091 uM to 2.097 uM; and on Day 5 the intracellular concentration is reduced to 1.294 uM.

With respect to NRP BCG exposed to varying concentrations of GSSG, we performed the intracellular ATP assay to determine that the NRP BCG cells are indeed viable, in addition to the BCG remaining in the NRP state and utilizing the same amount of ATP as unexposed NRP BCG. NRP BCG exposed to GSSG exhibit decreased intracellular ATP concentrations in comparison to mid-log BCG exposed to GSSG (Figure 7b). Unexposed NRP BCG on Day 1 presented an intracellular ATP concentration of 0.017 uM. A significant increase is noted on Day (0.476 uM), and Day 5 (0.697 uM), which is maintained into Day 5 (0.553 uM). NRP BCG exposed to 4 mM GSSG shows to have an increase in ATP over four days; 0.024 uM - 0.886 uM. On Day 5, a decrease is noted to 0.633 uM. In comparison to unexposed and 4 mM GSSG treated, 8 mM GSSG treated cells exhibited the greater free intracellular ATP concentrations. On Day 1, the concentration was 0.016 uM; a significant increase is occurs on Day 3 (0.683 uM), and a maximum on Day 4 (1.079 uM). A decrease in intracellular ATP concentration is noted on Day 5 (0.547 uM) by a factor of 1.97. Upon evaluation of cell energetics, all samples resulted in similar free ATP values over the five-day period. Taken together, these results confirm that the growth of NRP BCG is not affected by the exposure to GSSG.

M. bovis – BCG GSNO Results

In order to further investigate the effect of the final glutathione derivative, GSNO, we performed growth studies, cell viability plating, and intracellular ATP assays to determine its effects on mid-log and NRP BCG. Although not presented, mid-log and NRP BCG was exposed to 4 and 8 mM GSNO, over a five day period. These growth studies were evaluated similarly to that of GSH and GSSG. The growth curve, cell viability assay, and intracellular ATP assay results did not show statistically varying data when compared to that of GSSG. Figures 5, 6, and 7 can attest to the data presented by the GSNO studies. In addition, HPLC thiol analysis upon exposure to GSSG and GSNO has not been completed. The results from all three assays confirm that GSNO is only capable of inhibiting mid-log BCG cell growth, and has no effect on the growth and replication of NRP BCG.

Discussion

Influence of GSH on Mid-log and NRP BCG

Four distinct phases characterize the growth of bacteria over a period of time. These successive stages define the growth curve, which consists of a lag, log, stationary, and decline phases. Our results show that the mid-log BCG unexposed bacteria exhibit mid-logarithmic growth with approximately an eight-fold increase in optical density over the five days. This was similar to Mid-log BCG exposed to 4 mM GSH (Figure 1a). After evaluating the viability tests (Figure 2a) to confirm the bacteriostatic effects of 4 mM GSH, we conclude that *M. bovis*-BCG is capable of detoxifying 4 mM GSH, and is not detrimental to its growth. This is supported by the presence of quantified viable CFU over the five-day period. In addition, when evaluating the energetics of unexposed and 4 mM GSH exposed bacilli (Figure 3a), both cell trials followed similar patterns of ATP utilization over the five days. This data suggests that *M. bovis*-BCG growth is not inhibited by 4 mM GSH.

The growth of mid-log BCG was completely halted upon exposure to 8 mM GSH over five days (Figure 1a). The viability data shows quantifiable colony forming units on days 1, 2, and 3. However, in support of 8 mM GSH being toxic to BCG, there are no quantifiable colony forming units on days 4 and 5. The intracellular free-ATP quantization assay (Figure 3a) shows that there is a 17.5 fold increase in free intracellular ATP by Day 4. An up-regulation in genes and systems controlling these aspects of the cell, require an influx of free ATP. Therefore, over the four-day period, the cells are attempting the overcome the stress implemented by toxic levels of GSH. The second perspective emphasizes that toxicity due to GSH has already killed the bacterial cells. However, the cells have not lysed, resulting in an accumulation of ATP. The decrease in ATP levels on Day 5 can be explained by the lack of bacterial growth and replication due to consistent exposure to toxic concentrations of GSH. Although these three analyses collectively confirm that 8 mM GSH does kill mid-logarithmic, they fail to propose a definitive explanation as to how GSH is able to kill the cells. Previous studies have assessed the interaction of GSH with mid-log BCG have shown that Dpp and Opp transporters in the cell membrane of the bacteria uptake glutathione, or uptake cy-gly. These two components can be attributed to the toxicity of glutathione (8).

Nevertheless, no studies have been performed to determine the effects of GSH on NRP BCG. We performed a growth study over five days to evaluate the effect of GSH on the growth of NRP BCG. Our study revealed that unexposed NRP BCG remained in NRP and no conversion to mid-logarithmic growth was observed. The maximum OD_{600} obtained and maintained was approximately 0.135. Similarly, NRP BCG exposed to 4 mM GSH revealed no changes in growth, or exit from the NRP state. The maximum OD_{600} of 4 mM GSH exposed NRP BCG was 0.135. (Figure 1b). The inhibition and viability assays performed for unexposed and 4 mM GSH exposed NRP BCG show there are viable cells throughout the five days. In addition the viability indicates that there is no increase in the number of viable cells; suggesting that cells in both of these trials have remained in NRP. In relation to cell energetics, the initial concentration of free ATP in unexposed NRP BCG was 0.071 uM, and 0.024 uM in 4 mM GSH NRP BCG. Throughout the progression of the trail, unexposed NRP BCG did show increased levels of free ATP on days 3, 4, and 5; ranging between 0.746 uM and 1.698 uM. 4 mM GSH NRP BCG followed a similar increase in free intracellular ATP, but the concentrations ranged between

0.241 uM and 0.406 uM. This accumulation of ATP in the cell may be attributed to the regulation of the NRP state, ensuring the cells remain in NRP. Also, when the cells are in the NRP they have decreased metabolism, suggesting that this basal amount of ATP is necessary to keep the cell alive in the low metabolic state. The ATP assay was performed to confirm that the free ATP present in mid-log BCG is significantly greater than that in NRP BCG. Also, by evaluating the free ATP in mid-log and NRP determined whether the induced NRP state was maintained over the five days.

Our most significant findings reveal an unexpected growth of NRP BCG upon exposure to 8 mM GSH over five days. On Days 1, 2, and 3 the optical density remains within a standard deviation of 0.100. On Day 4, the optical density of the 8 mM GSH NRP BCG average increases to 0.207; a two fold increase in cell density. Furthermore, on Day 5, the average optical density increased to 0.398, also by a factor of two. This data presents an enigma as to how the bacteria are able to exit the NRP state, and enter active mid-logarithmic growth. Cell viability assays performed on NRP BCG revealed a ten fold lower number of cells in comparison mid-logarithmic bacterial cells. This is consistent with the models developed to explain the relative abundance of bacterial cells in active growth, and lack of active replication in latent mycobacteria (39). On Day 5, the viability assay (Figure 2b) indicates an increase in the number of CFU for unexposed, 4 mM GSH, and 8 mM GSH exposed NRP BCG. Upon normalization of the data for an OD_{600} of 0.100 (Figure 2c), the data shows there are viable cells in unexposed and 4 mM GSH NRP BCG. Thus, unexposed and 4 mM GSH BCG does not exit the NRP state. In contrast, the normalization of 8 mM GSH NRP BCG shows an approximate two fold decrease in the number of viable NRP mycobacteria. This data suggests that 8 mM GSH stimulates the transition from the NRP state to active mid-logarithmic growth. Once the mycobacteria have entered mid-log growth, 8 mM GSH acts to simultaneously kill the BCG. This killing is consistent with the killing data presented in our mid-log trials. In order to substantiate this claim, the energetics of the NRP BCG were evaluated over the five days. NRP mycobacteria exposed to 8 mM GSH showed to have basal free ATP levels of 0.016 – 0.045 uM. An increase in free ATP to 0.197 uM is noted on Day 3. Quantitatively, this is approximately a ten-fold increase in free ATP. On days 4 and 5, the intracellular free ATP levels returned to the basal as reported on days 1 and 2. This data supports the NRP exit because on Day 3, the increase in free intracellular ATP could potentially indicate that the cells are increasing their metabolic needs, in addition to various other cellular regulatory processes, to exit the NRP state. On days 4 and 5 the ATP levels return back to normal because this ATP is being utilized. However, on Day 5, it is hypothesized that the cells are in mid-logarithmic growth, and 8 mM GSH acts to kill the mycobacteria; thus explaining the decreased free intracellular ATP levels.

Previously, it has been hypothesized that GSH acts to create an oxidative imbalance within the mycobacterial cell, resulting in cell death (7). Currently, thiol HPLC analysis studies are being performed to determine the overall mycobacterial oxidative state of mid-log BCG exposed to 8 mM GSH. The results from the NRP HPLC mycothiol analysis (Figure 4d), show on Day 4 a decrease in mycothiol concentration in 8 mM GSH NRP BCG cells. This decrease in mycothiol may be suggestive of a mechanism or response from exposure to GSH, leading to exit from the NRP state. However, no studies have been performed to evaluate whether the changes in the oxidative state of the NRP cytoplasm facilitate the exit from the NRP state.

In order to fully evaluate the exit from NRP, the DosR regulation mechanism must be taken into account. Over the five days, the design of the protocol exposes the bacteria to a minimal, but uncalculated low concentration of oxygen. In order to maintain a hypoxic environment, sterile glass beads are added to reduce the headspace of free available oxygen in each culture tube, consistently over five days. Other procedures use more advanced molecular techniques to ensure that the mycobacteria remain in the NRP state by exposing them to low non-toxic concentrations of CO or NO (38). These molecules occupy the binding site of the DosR system, initiating and 'locking' the transition into latency. Once bound, due to binding affinities, these molecules cannot be displaced, even in the presence of environmental oxygen. When manipulating the Wayne model for NRP, latency is achieved by extended non-shaking incubation, which eventually creates an anoxic environment through activation of the DosR regulon. When no oxygen molecules are eventually binding onto the DosR binding site, the latency genes are successively upregulated – inducing NRP. The introduction of low concentrations of oxygen can potentially allow binding to the DosR system at the heme group of DosT, reversing the process, and promoting exit from the NRP state. We hypothesize that the introduction of low concentrations of oxygen coupled with the activity of GSH (although unknown) induces exit from the NRP state. Furthermore, these results suggest that GSH can act or mimic a direct or indirect inducer for pathways associated with the regulation of the NRP state.

Influence of GSSG/GSNO on Mid-log and NRP BCG

The oxidized form of glutathione (GSSG) was also tested against mid-log and NRP BCG over five days to assess the impact of the compound on both cell stages. Mid-log BCG exposed to 4 and 8 mM GSSG presented data similar to that of mid-log BCG exposed to GSH (Figure 5a). The growth curve, cell viability assay, and intracellular ATP assay have collectively confirmed that that GSSG inhibits cell growth, but is not able to kill the cells.

NRP BCG exposed to 4 and 8 mM GSSG revealed no deviation in the growth curve in comparison to unexposed NRP BCG (Figure 5b). Over the five day trial period, the OD_{600} increased from 0.100 (Day 1) to 0.249 (Day 5) for all three sample types. The cell viability assay results show there are similar cell units in each sample progressively over the five days (Figure 6b). These data are indicative of neither bacterial growth stimulation nor killing.

Growth studies, cell viability assays, and cell energetic assays were performed for mid-log and NRP BCG exposed to 4 and 8 mM GSNO. However, due to similarity of results with mid-log and NRP BCG exposed to GSSG, the data is not presented. Similar to that of mid-log BCG, GSNO showed to inhibit the growth over five days; killing due to exposure was not confirmed. Also, NRP BCG exposed to GSNO showed to have no deviation in results when compared to unexposed NRP BCG.

Acknowledgements

We gratefully acknowledge the American Society for Microbiology – Undergraduate Research Fellowship (2011), Pace University Undergraduate Research Initiative (2011), Pace University Pforzheimer Honors College Research Grant (2012), and Pace University Dyson Summer Research Grant (2011) for providing the funds to enable the completion of this research. In addition, we would like to recognize and acknowledge the Pace University Department of Biology and Health Sciences for providing the research facility and equipment for the growth, viability, and ATP studies. In addition, we would like to recognize and thank Nigel Yarlett PhD – Director of Haskins Laboratories for providing us with the equipment, facility, advise, and help related to the completion of the HPLC analysis.

References

1. Armstrong J.A., Hart P. D. 1971. "Response of cultured macrophages to Mycobacterium tuberculosis, with observations on fusion of lysosomes with phagosomes," The Journal of Experimental Medicine, vol. 134, no. 3, pp. 713–740.
2. Attarian, R., Bennie, C., Bach, H., and Av-Gay, Y. 2009. Glutathione disulfide and S-nitrosoglutathione detoxification by *Mycobacterium tuberculosis* thioredoxin system. *FEBS Lett*. 583:3215-3220.
3. Balázsi, G., A. P. Heath, L. Shi, and M. L. Gennaro. 2008. The temporal response of the *Mycobacterium tuberculosis* gene regulatory network during growth arrest. Mol. Syst. Biol. 4225.
4. Betts, J.C., P.T. Lukey, L.C. Robb, R.A. McAdam, and K. Duncan. 2002. Evaluation of a nutrient starvation model of Mycobacterium tuberculosis persistence by gene and protein expression profiling. Mol. Microbiol. 43:717–731.
5. Buchmeier NA, Newton GL, Koledin T, Fahey RC. 2003. Association of mycothiol with protection of Mycobacterium tuberculosis from toxic oxidants and antibiotics. *Molecular Microbiology* 46;1723-32.
6. Cho, H. Y., H. J. Cho, Y. M. Kim, J. I. Oh, and B. S. Kang. 2009. Structural insight into the heme-based redox sensing by DosS from *Mycobacterium tuberculosis*. J. Biol. Chem. 28413057-13067.
7. Connell ND, Venketaraman V. 2009. Control of *Mycobacterium tuberculosis* Infection by Glutathione. Recent Patents on Anti-Infective *Drug Discovery* (4):214-26.
8. Dasgupta A, Sureka K, Mitra D, Saha B, Sanyal S, et al. (2010) An Oligopeptide Transporter of Mycobacterium tuberculosis Regulates Cytokine Release and Apoptosis of Infected Macrophages. PLoS ONE 5(8): e12225. doi:10.1371/journal.pone.0012225.
9. Dayaram, Y.K., Talaue, M.T., Connell, N.D. and Venketaram, V. 2006. Characterization of a Glutathione Metabolic Mutant of *Mycobacterium tuberculosis* and its Resistance to Glutathione and Nitrosoglutathione. *J. Bacteriol*. 188:1364-1372.
10. De Groote, M. A., D. Granger, Y. Xu, G. Campbell, R. Prince, and F. C. Fang. 1995. Genetic and redox determinants of nitric oxide cytotoxicity in a Salmonella typhimurium model. Proc. Natl. Acad. Sci. USA 92:6399–6403.
11. Deneke SM, Fanburg BL. Regulation of cellular glutathione. Am J Physiol 1989; 257(4 Pt 1): L163-173.
12. England K, Crew R, Slayden R. 2011. *Mycobacterium tuberculosis* septum site determining protein, Ssd encoded by Rv3660c, promotes filamentation and elicits an alternative metabolic and dormancy stress response. *BMC Microbiology* 11;79.
13. Fahey RC, Newton GL (1987) Determination of low-molecular- weight thiols using monobromobimane fluorescent labeling and high-performance liquid chromatography. Methods Enzy- mol 143:85–96.
14. Fontan, P., Aris, V., Ghanny, S., Soteropoulos, P., Smith, I. 2008. Global Transcriptional Profile of *Mycobacterium tuberculosis* During THP-1 Human Macrophage Infection. *Infect Immun*. 76(2):717-25.
15. Green, R.M., Seth, A., and Connell, N.D. 2000. A Peptide Permease Mutant of *Mycobacterium bovis*-BCG Resistant to the Toxic Peptides Glutathione and *S*-Nitrosoglutathione. *Infec. Immunol.* 68:429-436.
16. Griffith OW. Biologic and pharmacologic regulation of mammalian glutathione synthesis. Free Radic ATTN: Biol Med 1999; (9-10): 922-935.

17. Honaker RW, Leistikow RL, Bartek IL, Voskuil MI: Unique roles of DosT and DosS in DosR regulon induction and Mycobacterium tuberculosis dormancy**.** *Infect Immun* 2009, 77(8)**:**3258-3263.
18. Hu, Y., Coates A.R.M., and Mitchison, D.A. (2003) Sterilizing Activities of Fluoroquinolones Against Rifampin-Tolerant Populations of *M. tuberculosis.* Antimicrob. Agents Chermother. 47:653-657.
19. Kumar, A., J. C. Toledo, R. P. Patel, J. R. Lancaster, Jr., and A. J. Steyn. 2007. *Mycobacterium tuberculosis* DosS is a redox sensor and DosT is a hypoxia sensor. Proc. Natl. Acad. Sci. USA 10411568-11573.
20. Kumar, A., J. S. Deshane, D. K. Crossman, S. Bolisetty, B. S. Yan, I. Kramnik, A. Agarwal, and A. J. Steyn. 2008. Heme oxygenase-1 derived carbon monoxide induces the *Mycobacterium tuberculosis* dormancy regulon. J. Biol. Chem. 28318032-18039.
21. Lee, J. M., H. Y. Cho, H. J. Cho, I. J. Ko, S. W. Park, H. S. Baik, J. H. Oh, C. Y. Eom, Y. M. Kim, B. S. Kang, and J. I. Oh. 2008. O_2 and NO sensing mechanism through the DevSR two-component system in *Mycobacterium smegmatis*. J. Bacteriol. 1906795-6804.
22. Lu, S., P. B. Killoran, F. C. Fang, and L. W. Riley. 2002. The global regulator ArcA controls resistance to reactive nitrogen and oxygen intermediates in Salmonella enterica serovar Enteritidis. Infect. Immun. 70:451–461.
23. Manca, C., Paul, S., Barry 3rd, C.E., Freedman, V.H. and Kaplan, G. (1999). Mycobacterium tuberculosis catalase and peroxidase activities and resistance to oxidative killing in human monocytes in vitro. Infect. Immun. 67, 74–79.
24. Newton GL, Arnold K, Price MS, Sherrill C, delCardayré SB, Aharonowitz Y, Cohen G, Davies J, Fahey RC, Davis C (1996) Distribution of thiols in microorganisms: Mycothiol is a major thiol in most actinomycetes. J Bacteriol 178:1990–1995
25. Nikitovic, D., and A. Holmgren. 1996. S-nitrosoglutathione is cleaved by the thioredoxin system with liberation of glutathione and redox regulating nitric oxide. J. Biol. Chem. 271:19180–19185.
26. Penninckx, M. J., and M. T. Elskens. 1993. Metabolism and functions of glutathione in micro-organisms. Adv. Microb. Physiol. 34:239–301.
27. Roberts, D. M., R. P. Liao, G. Wisedchaisri, W. G. Hol, and D. R. Sherman. 2004. Two sensor kinases contribute to the hypoxic response of *Mycobacterium tuberculosis*. J. Biol. Chem. 27923082-23087.
28. Saini, D. K., V. Malhotra, and J. S. Tyagi. 2004. Cross talk between DevS sensor kinase homologue, Rv2027c, and DevR response regulator of *Mycobacterium tuberculosis*. FEBS Lett. 56575-80.
29. Sardiwal, S., S. L. Kendall, F. Movahedzadeh, S. C. Rison, N. G. Stoker, and S. Djordjevic. 2005. A GAF domain in the hypoxia/NO-inducible *Mycobacterium tuberculosis* DosS protein binds haem. J. Mol. Biol. 353929-936.
30. Saunders BM, Britton WJ. 2007. Life and death in the granuloma: Immunopathology of tuberculosis. Immunology and Cell Biology :103-11.
31. Sherman, D. R., M. Voskuil, D. Schnappinger, R. Liao, M. I. Harrell, and G. K. Schoolnik. 2001. Regulation of the *Mycobacterium tuberculosis* hypoxic response gene encoding α-crystallin. Proc. Natl. Acad. Sci. USA 987534-7539.
32. Shiloh, M. U., P. Manzanillo, and J. S. Cox. 2008. *Mycobacterium tuberculosis* senses host-derived carbon monoxide during macrophage infection. Cell Host Microbe 3323-330.
33. Sousa, E. H., J. R. Tuckerman, G. Gonzalez, and M. A. Gilles-Gonzalez. 2007. DosT and

DevS are oxygen-switched kinases in *Mycobacterium tuberculosis*. Protein Sci. 161708-1719.
34. Stover, C. K., V. F. de la Cruz, T. R. Fuerst, J. E. Burlein, L. A. Benson, L. T. Bennett, G. P. Bansal, J. F. Young, M. H. Lee, G. F. Hatfull, et al. 1991. New use of BCG for recombinant vaccines. Nature 351456-460.
35. Ulrichs T, Kaufmann S. 2006. New Insights Into the Function of Granulomas in Human Tuberculosis. J Pathol; 208: 261–269.
36. Ung, K.S. and Av-Gay, Y. (2006) Mycothiol-dependent mycobacterial response to oxidative stress. FEBS Lett. 580, 2712–2716.
37. Van Crevel R., Ottenhoff T.H.M., and Van derMeer J.W.M. 2002 "Innate Immunity to Mycobacterium tuberculosis,' Clinical Microbiology Reviews, Vol. 15, No. 2, PP. 294-309.
38. Voskuil MI, Schnappinger D, Visconti KC, Harrell MI, Dolganov GM, Sherman DR, Schoolnik GK. 2003. Inhibition of respiration by nitric oxide induces a Mycobacterium tuberculosis dormancy program. J Exp Med.;198(5):705-13.
39. Wayne, L. G., and K. Y. Lin. 1982. Glyoxylate metabolism and adaptation of Mycobacterium tuberculosis to survival under anaerobic conditions. Infect. Immun. 37:1042–1049.
40. Wayne, L.G. and Sohaskey, C.D. 2001 . Nonreplicating Persistance of *Mycobacterium tuberculosis*. *Annu. Rev. Microbiol*. 55:139-163.
41. Wooff E, Michell SL, Gordon SV, Chambers MA, Bardarov S, Jacobs WR Jr, Hewinson RG, Wheeler PR. 2002. Functional genomics reveals the sole sulphate transporter of the Mycobacterium tuberculosis complex and its relevance to the acquisition of sulphur in vivo. Mol Microbiol. Feb;43(3):653-63.
42. Yuan, Y., D. D. Crane, R. M. Simpson, Y. Q. Zhu, M. J. Hickey, D. R. Sherman, and C. E. Barry, 3rd. 1998. The 16-kDa α-crystallin (Acr) protein of *Mycobacterium tuberculosis* is required for growth in macrophages. Proc. Natl. Acad. Sci. USA 959578-9583.
43. Zhang, Y., Lathigra, R., Garbe, T., Catty, D. and Young, D. (1991) Genetic analysis of superoxide dismutase, the 23 kDa antigen of Mycobacterium tuberculosis. Mol. Microbiol. 5, 381–391.

Figure Legends

Figure 1a. Growth Curve of Mid-log BCG Exposed to GSH. The mid-log BCG GSH growth curve shows upon exposure to 8 mM GSH over five days, the OD_{600} does not exceed 0.25. Unexposed mycobacteria reach a maximum OD_{600} of 0.80 over five days. No significant deviations are noted for mycobacteria exposed to 4 mM GSH in comparison to unexposed mycobacteria.

Figure 1b. Growth Curve of NRP BCG Exposed to GSH. Unexposed NRP BCG reached a maximum OD_{600} of 0.15 over five days. NRP BCG exposed to 4 mM GSH reached a maximum OD_{600} of 0.15, mimicking that of unexposed mycobacteria. Exposure to 8 mM GSH, NRP BCG increased in OD_{600} from 0.10 (Day 1) to 0.40 (Day 5).

Figure 2a. Total Bacterial Cell Count of Mid-log BCG Exposed to GSH. This cell viability assay reports quantifiable CFU through day three for unexposed, 4 and 8 mM GSH exposed mycobacteria. On Day four and five, no viable CFU were quantitated upon exposure to 8 mM GSH. The lateral axis is scaled to a maximum of 7.0×10^9. This represents the number of viable cells in the overall culture tube; not normalized to OD_{600} of 0.1.

Figure 2b. Total Bacterial Cell Count of NRP BCG Exposed to GSH. This data represents the CFU quantification for unexposed, 4 mM and 8 mM GSH NRP BCG over five days. The data here is scaled to a maximum of viable cells present in the culture tube over five days. Note the lateral axis of the graph to be 6.0×10^8 (This is 10 fold smaller than that of Figure 2a). Primary region of focus is Day 5, where are substantially more viable bacteria present.

Figure 2c. Normalization of NRP BCG Exposed to GSH on Day 5 to OD_{600} = 0.1. Normalization of Day 5 data from Figure 2b is shown, to determine the number of viable CFU at an OD_{600} of 0.1. This data is shown for comparison reasons to determine the number of viable bacterial cells present in the 8 mM GSH NRP BCG on Day 5 as shown in Figure 2b. Note that the later axis of this graph extends to 6.0×10^8.

Figure 3a. Total Concentration of Free Intracellular ATP In Mid-log BCG Exposed to GSH. The results shown here represent the free intracellular cytoplasmic concentration of ATP in mid-log BCG over five days. Unexposed BCG had a maximum concentration of 1.38 μM over five days. BCG exposed to 8 mM GSH resulted in a maximum ATP concentration of 2.28 μM on Day four. On Day five, the intracellular ATP concentration of 8 mM exposed BCG decreased to 0.78 μM. 4 mM exposed BCG reached a maximum intracellular ATP concentration of 0.88 μM on Day two. All data present represents cell cultures normalized to OD_{600} 0.1.

Figure 3b. Total Concentration of Free Intracellular ATP In NRP BCG Exposed to GSH. Intracellular cytoplasmic ATP concentration for unexposed NRP BCG increased to a maximum of 1.70 μM on Day three. NRP BCG exposed to 4 mM GSH showed to have increased concentrations of intracellular ATP; 0.4 μM between Days three to five. NRP BCG exposed to 8 mM GSH did not reveal a significant increase in intracellular ATP over the five-day period. All data present represents cell cultures normalized to OD_{600} 0.1.

Figure 4a. HPLC Mycothiol Analysis of NRP BCG Control on Day 1. This chromatogram shows the thiol separation of Day 1 bacterial cells for unexposed bacteria, normalized to an OD_{600} of 0.1. This sample was separated using 0.25% Acetic Acid (pH of 4.2). The average retention times for the two regions are 12:36 minutes, and 18:52 minutes. Regions after 30 minutes are ghost peaks consistent with the media and other possible compounds. Regions of interest include Region 2 (Cys-Gly/L-Cys) and Region 3 (Mycothiol). The average retention time for Region 2 is 12.36 minutes; and for Region 3 it is the average retention time is 18:52 minutes.

Figure 4b. HPLC Mycothiol Analysis of NRP BCG Control on Day 5. The present chromatogram represents thiol separation of unexposed NRP BCG on Day 5, normalized to an OD_{600} of 0.1. This sample was analyzed using 0.25% Acetic Acid (pH of 4.2). The regions on interest include Region 2 (Cys-Gly/L-Cys) and Region 3 (Mycothiol). The average retention times for the two regions are 12:36 minutes, and 18:52 minutes. Regions after 30 minutes are ghost peaks consistent with the media and other possible compounds.

HPLC Analysis of Cys-Gly, GSH, and MSH in NRP BCG Exposed to GSH on Day 5. NRP BCG exposed to 8 mM GSH are separated using the HPLC thiol analysis method above. This chromatogram represents the separation of exposed NRP BCG using 0.25% Acetic Acid (pH 4.2). The sample was normalized to OD_{600} of 0.1. The average retention times for the two regions are 12:36 minutes, and 18:52 minutes. Regions after 30 minutes are ghost peaks consistent with the media and other possible compounds. Regions of interest include 2 (Cys-Gly/L-Cys), 2a (GSH/Cys-Gly/L-Cys), and 3 (Mycothiol). The average retention times for the three regions are 12:36 minutes, 14:55 minutes, and 18:52 minutes.

Figure 4d. Changes In the Amount of MSH Present In NRP BCG Exposed to GSH Over 5 Days. This graph plots the average areas of Region 3 (Mycothiol) over five days to assess the increase or decrease in cellular concentrations. The red line represents mycothiol concentrations in 8 mM GSH exposed cells, while the blue represent the average mycothiol concentration change over five days.

Figure 5a. Growth Curve of Mid-log BCG exposed to GSSG. The mid-log BCG GSSH growth curve shows upon exposure to 8 mM GSH over five days, the OD_{600} does not exceed 0.24. Unexposed mycobacteria reach a maximum OD_{600} of 0.77 over five days. No significant deviations are noted for mycobacteria exposed to 4 mM GSH in comparison to unexposed mycobacteria. OD_{600} for 4 mM GSSG exposed does not exceed 0.31.

Figure 5b. Growth Curve of NRP BCG exposed to GSSG. Unexposed NRP BCG reached a maximum OD_{600} value of 0.23, over five days. NRP BCG exposed to 4 mM GSSG increased to a maximum OD_{600} of 0.24 over five days. 8 mM GSSG NRP BCG showed a maximum increase in OD_{600} to 0.28 over the five-day period. These data show that there is no significant deviation between unexposed, 4, and 8 mM GSSG exposed NRP BCG.

Figure 6a. Total Bacterial Cell Count of Mid-log BCG Exposed to GSSG. This cell viability assay reports quantifiable CFU for unexposed, 4 and 8 mM GSSG exposed mid-log mycobacteria over five days. There is no significant deviation for the number of CFU present for

unexposed, 4, and 8 mM GSSG samples. All data present represent cell cultures normalized to an OD_{600} of 0.1.

Figure 6b. Total Bacterial Cell Count of NRP BCG Exposed to GSSG. This NRP BCG cell viability figure shows the quantization of CFU for unexposed, 4, and 8 mM GSSG. Over the five-day period, there is no significant difference in the number of CFU between all three trial conditions. All data present represent cell cultures normalized to an OD_{600} of 0.1.

Figure 7a. Total Concentration of Free Intracellular ATP In Mid-log BCG Exposed to GSH. The results shown here represent the free intracellular cytoplasmic concentration of ATP in mid-log BCG over five days. Unexposed BCG had a maximum concentration of 1.31 μM (Day 4) over five days. BCG exposed to 8 mM GSH resulted in a maximum ATP concentration of 2.10 μM on Day 4. 4 mM exposed BCG reached a maximum intracellular ATP concentration of 1.72 μM on Day 4. No statistical variation is noted in the data shown for unexposed, 4, and 8 mM GSSH exposed bacteria. All data present represents cell cultures normalized to OD_{600} 0.1.

Figure 7b. Total Concentration of Free Intracellular ATP In NRP BCG Exposed to GSH. The results shown here represent the free intracellular cytoplasmic concentration of ATP in NRP BCG over five days. Unexposed BCG had a maximum concentration of 0.70 μM (Day 4) over five days. BCG exposed to 8 mM GSH resulted in a maximum ATP concentration of 1.08 μM on Day 4. 4 mM exposed BCG reached a maximum intracellular ATP concentration of 0.89 μM on Day 4. No statistical variation is noted in the data shown for unexposed, 4, and 8 mM GSSH exposed bacteria. All data present represents cell cultures normalized to OD_{600} 0.1.

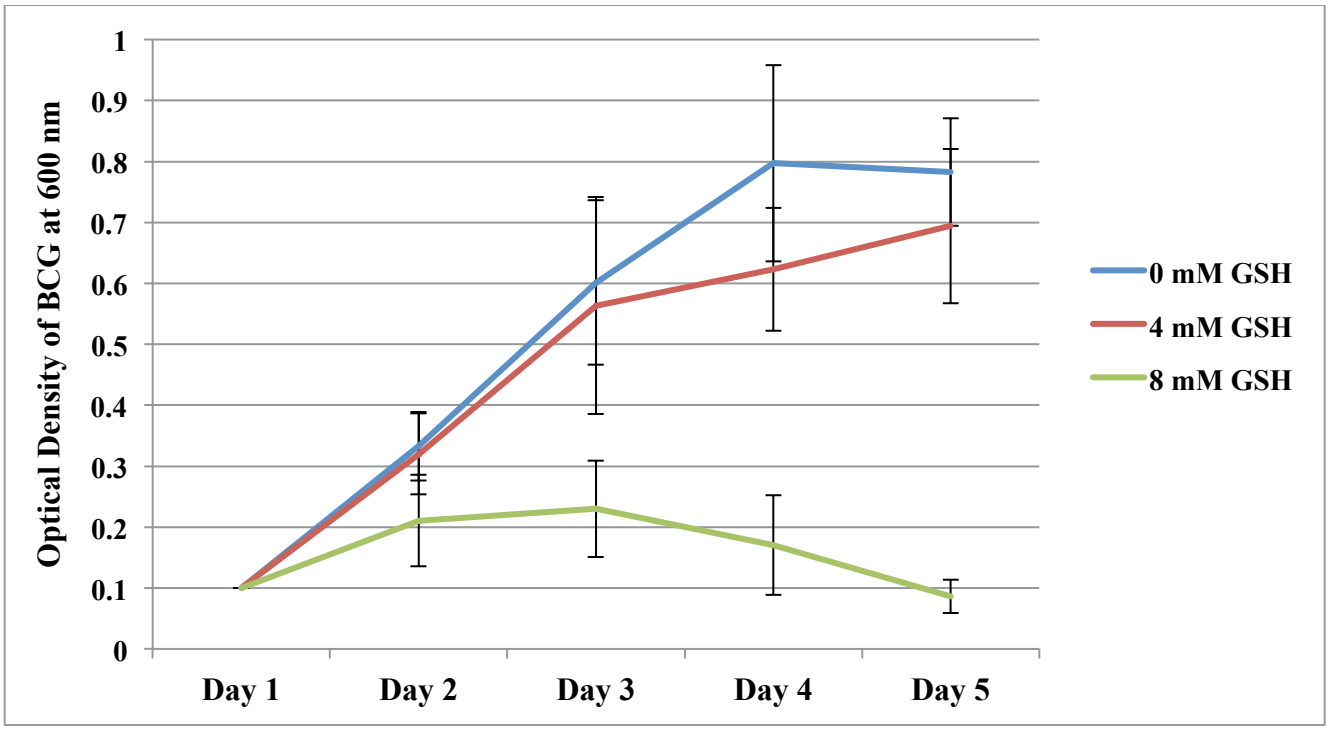

Figure 1a. Growth Curve of Mid-log BCG Exposed to GSH.

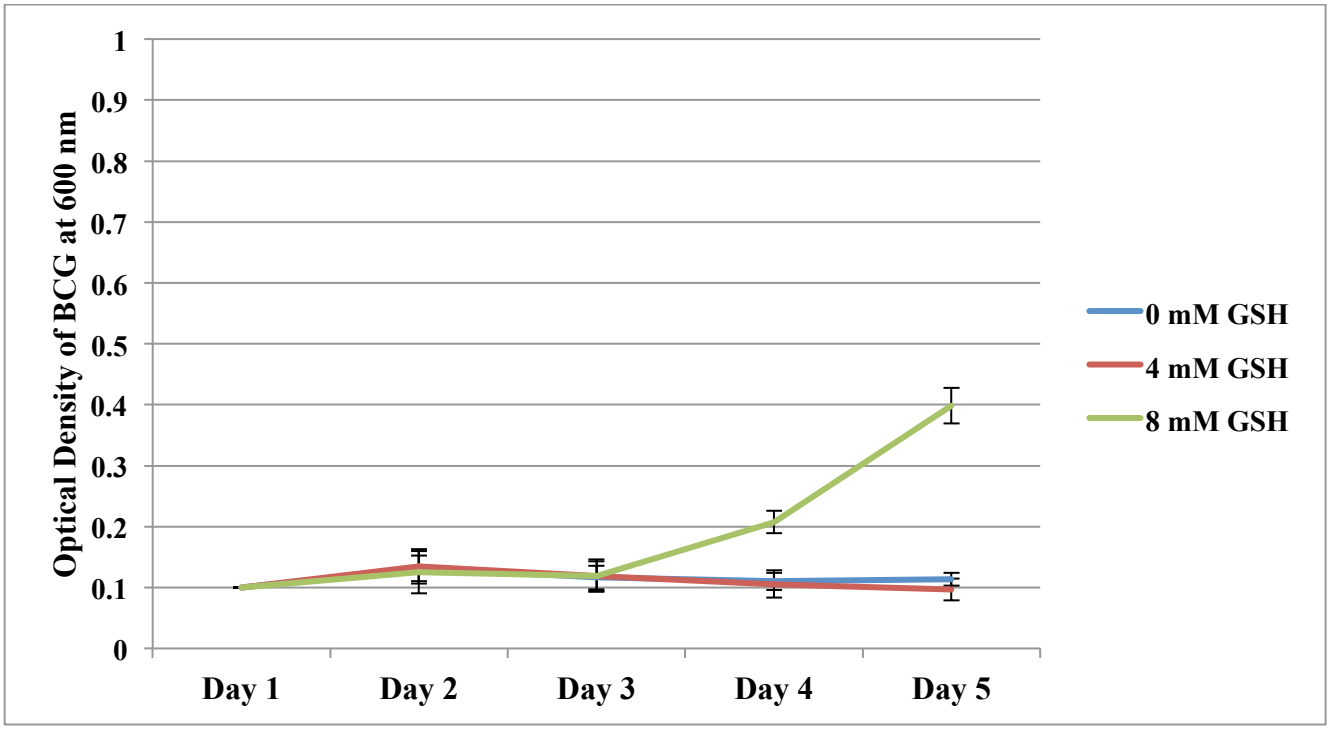

Figure 1b. Growth Curve of NRP BCG Exposed to GSH.

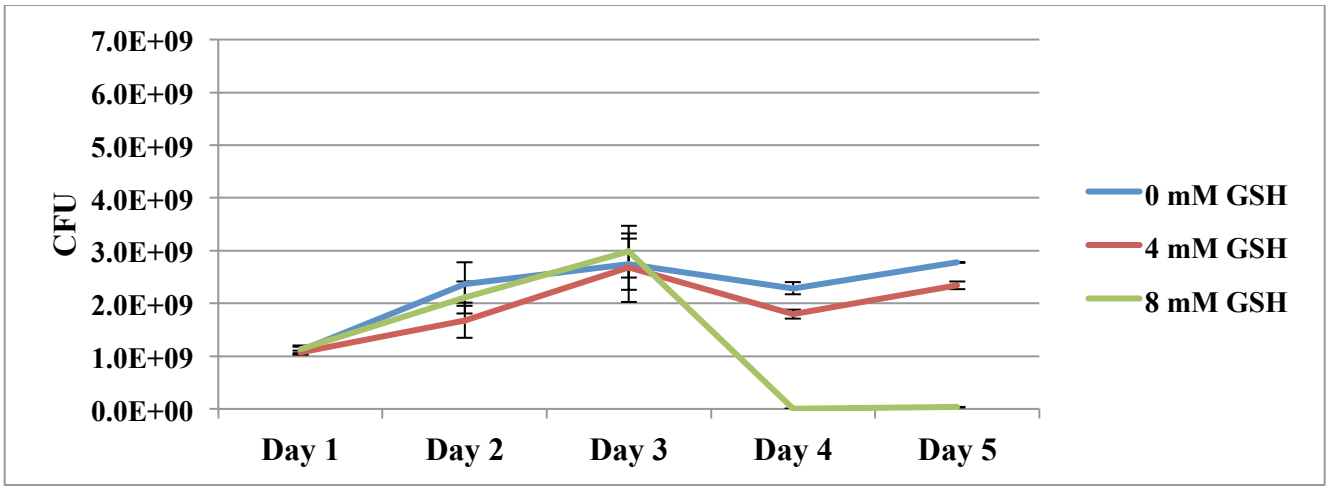

Figure 2a. Total Bacterial Cell Count of Mid-log BCG Exposed to GSH.

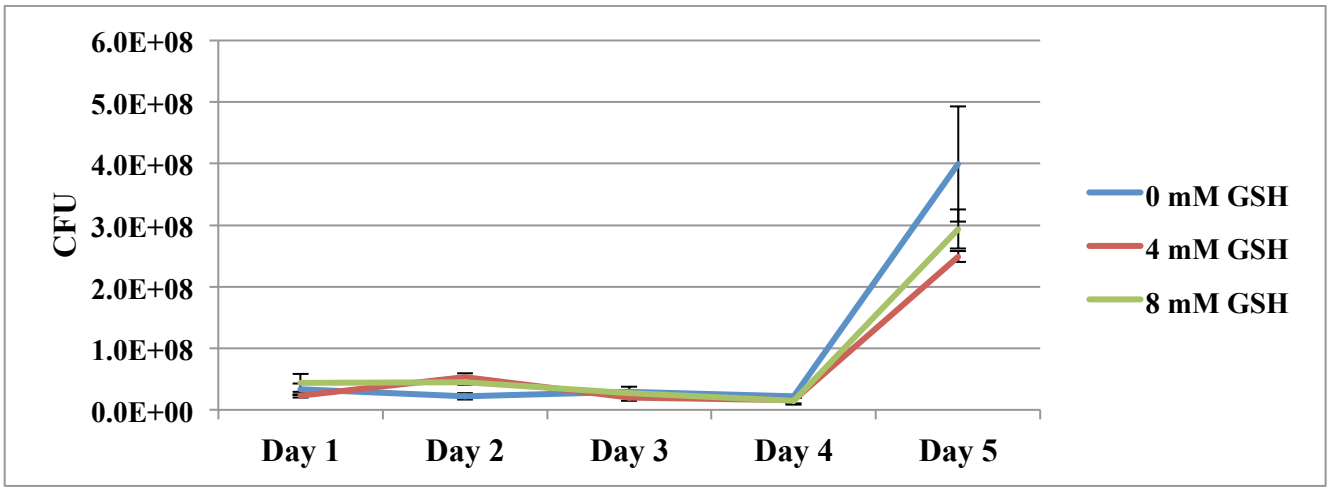

Figure 2b. Total Bacterial Cell Count of NRP BCG Exposed to GSH.

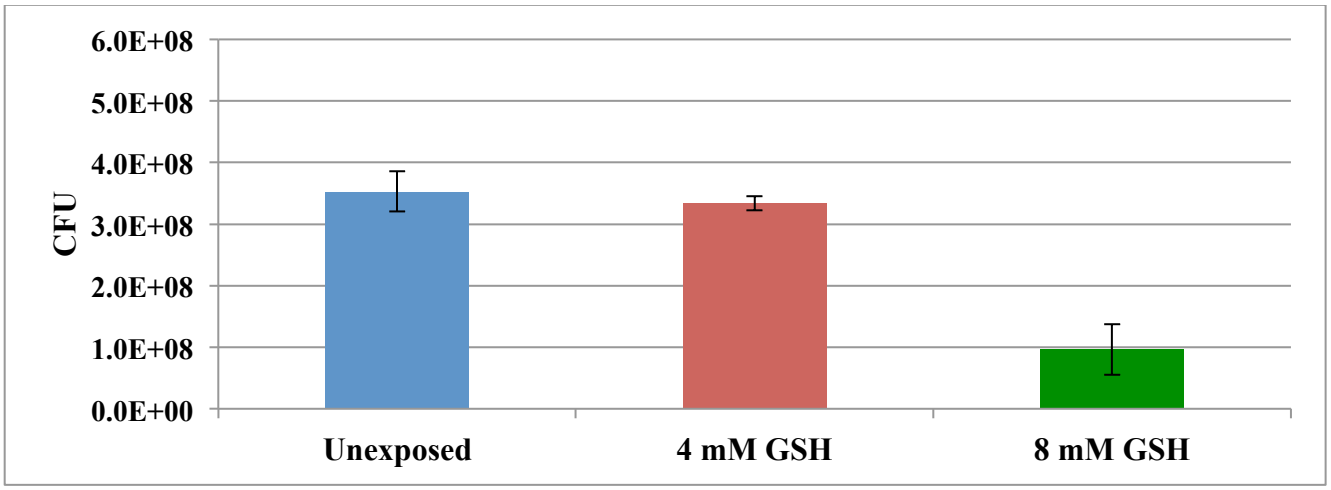

Figure 2c. Normalization of NRP BCG Exposed to GSH on Day 5 to OD_{600} = 0.1.

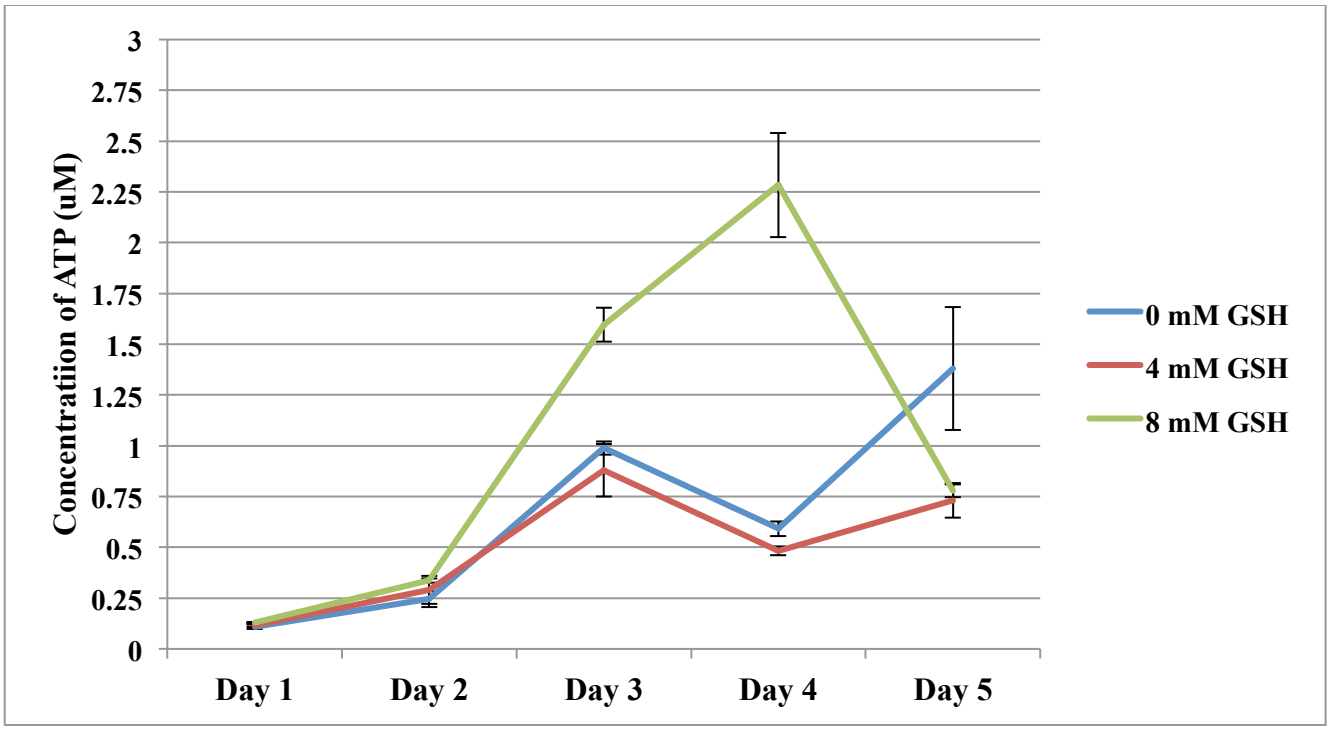

Figure 3a. Total Concentration of Free Intracellular ATP In Mid-log BCG Exposed to GSH.

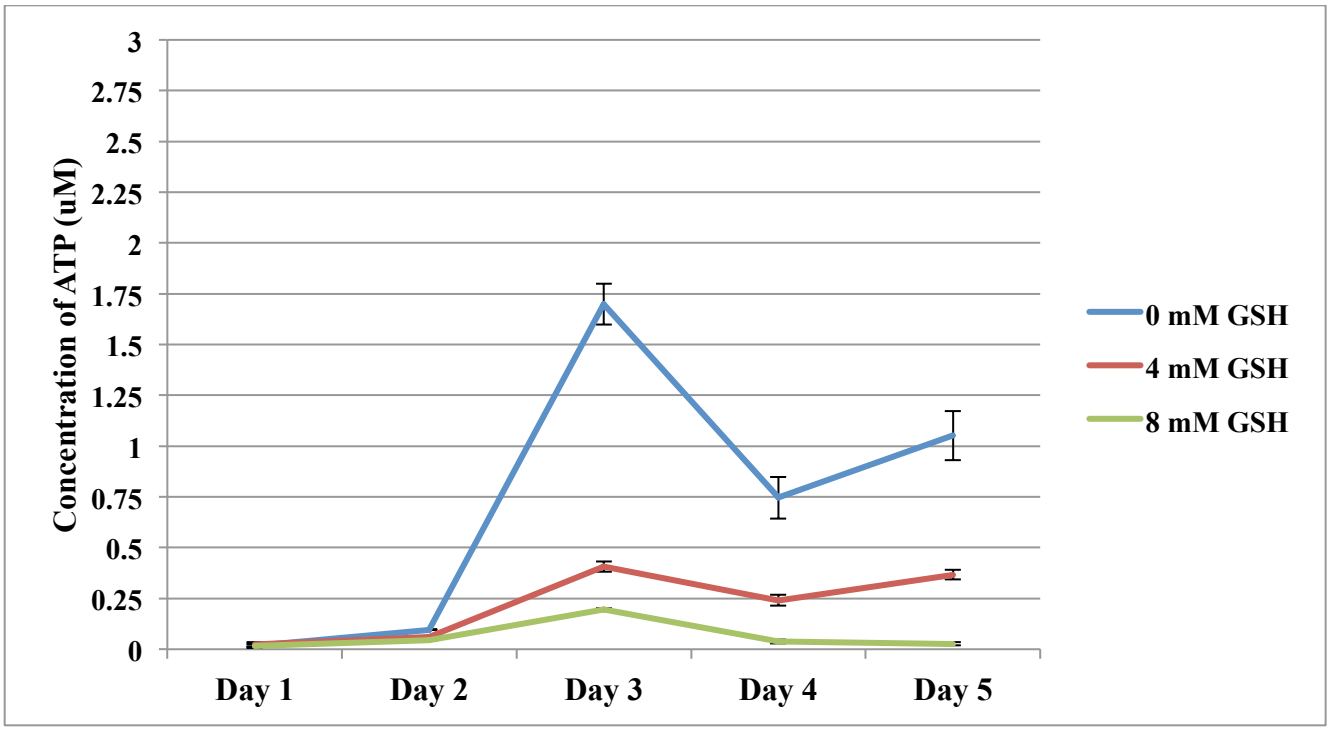

Figure 3b. Total Concentration of Free Intracellular ATP In NRP BCG Exposed to GSH.

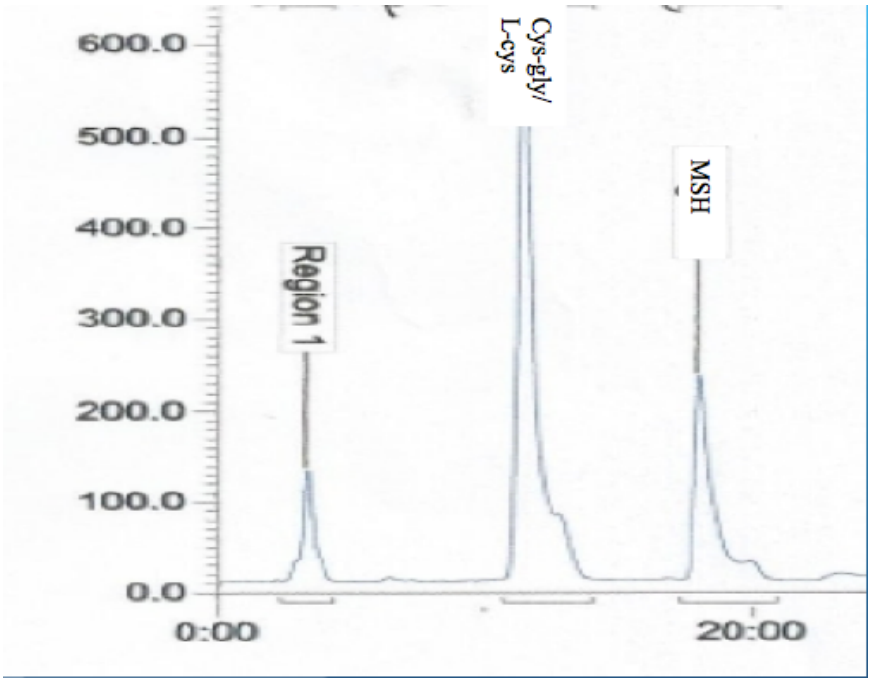

Figure 4a. HPLC Mycothiol Analysis of NRP BCG Control on Day 1.

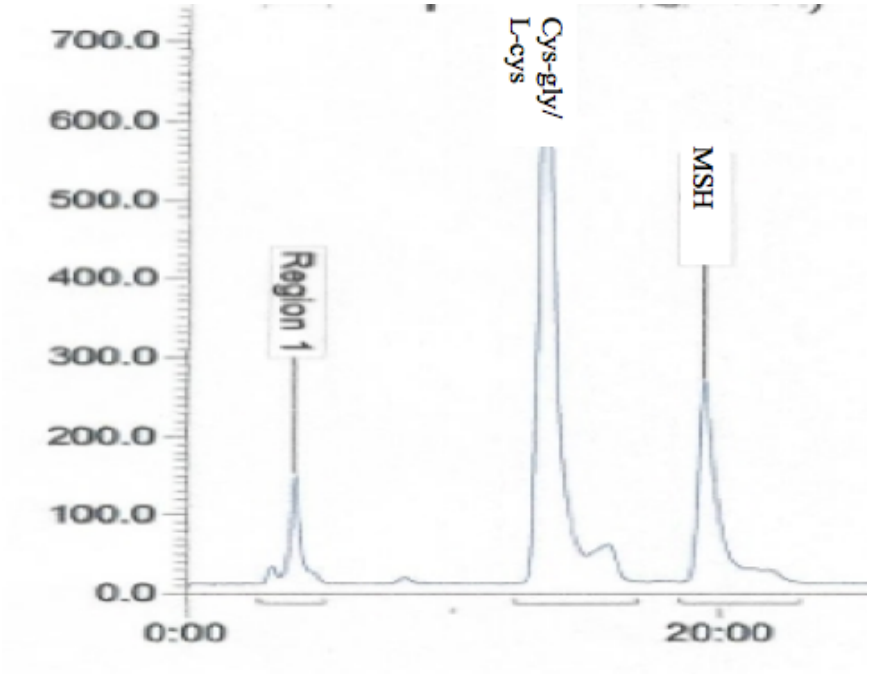

Figure 4b. HPLC Mycothiol Analysis of NRP BCG Control on Day 5.

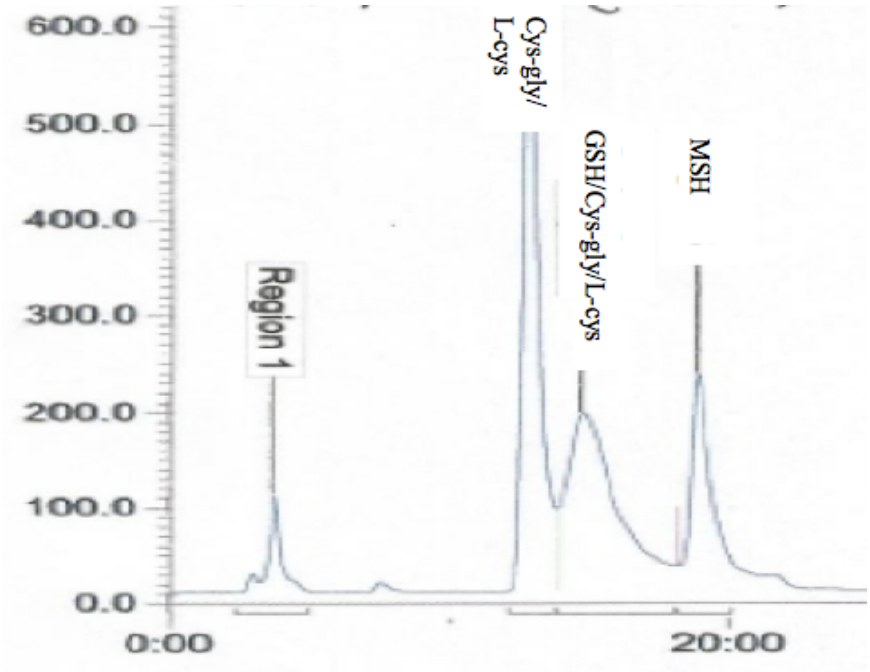

Figure 4c. HPLC Analysis of Cys-Gly, GSH, and MSH in NRP BCG Exposed to GSH on Day 5.

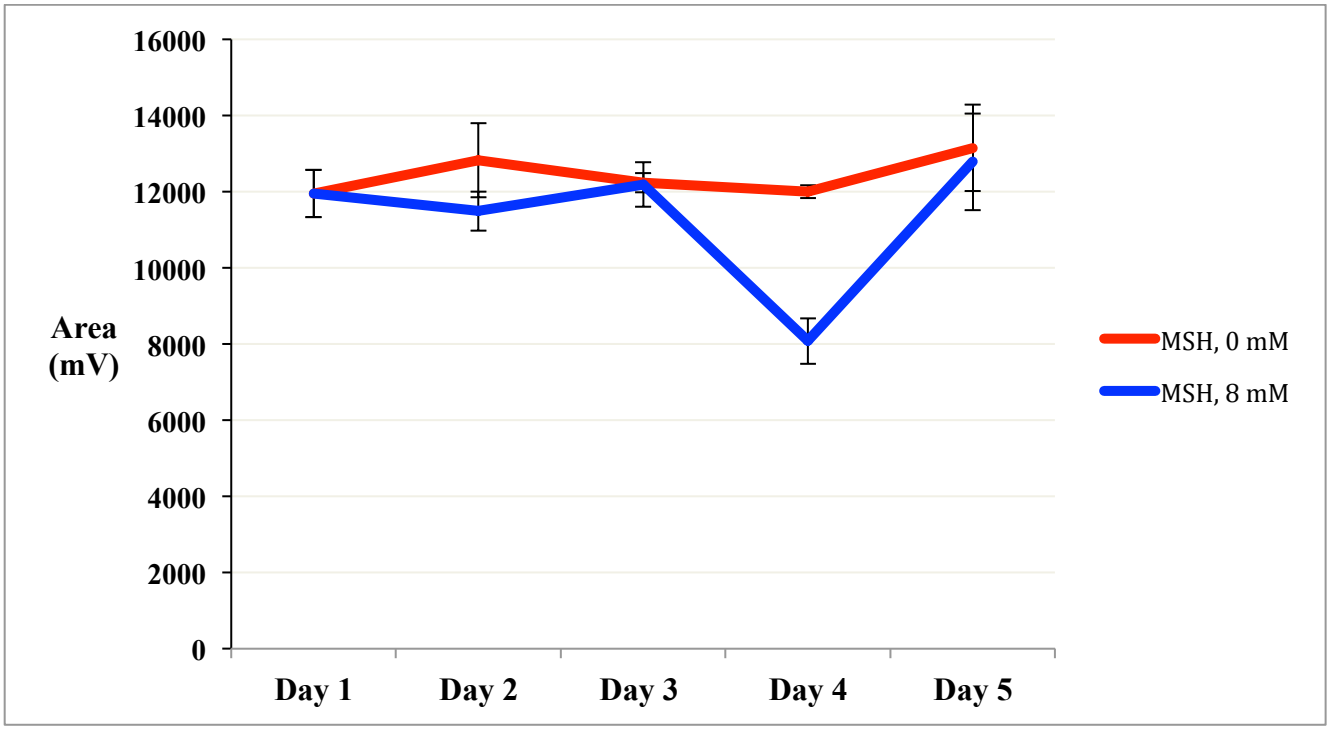

Figure 4d. Changes In the Amount of MSH Present In NRP BCG Exposed to GSH Over 5 Days.

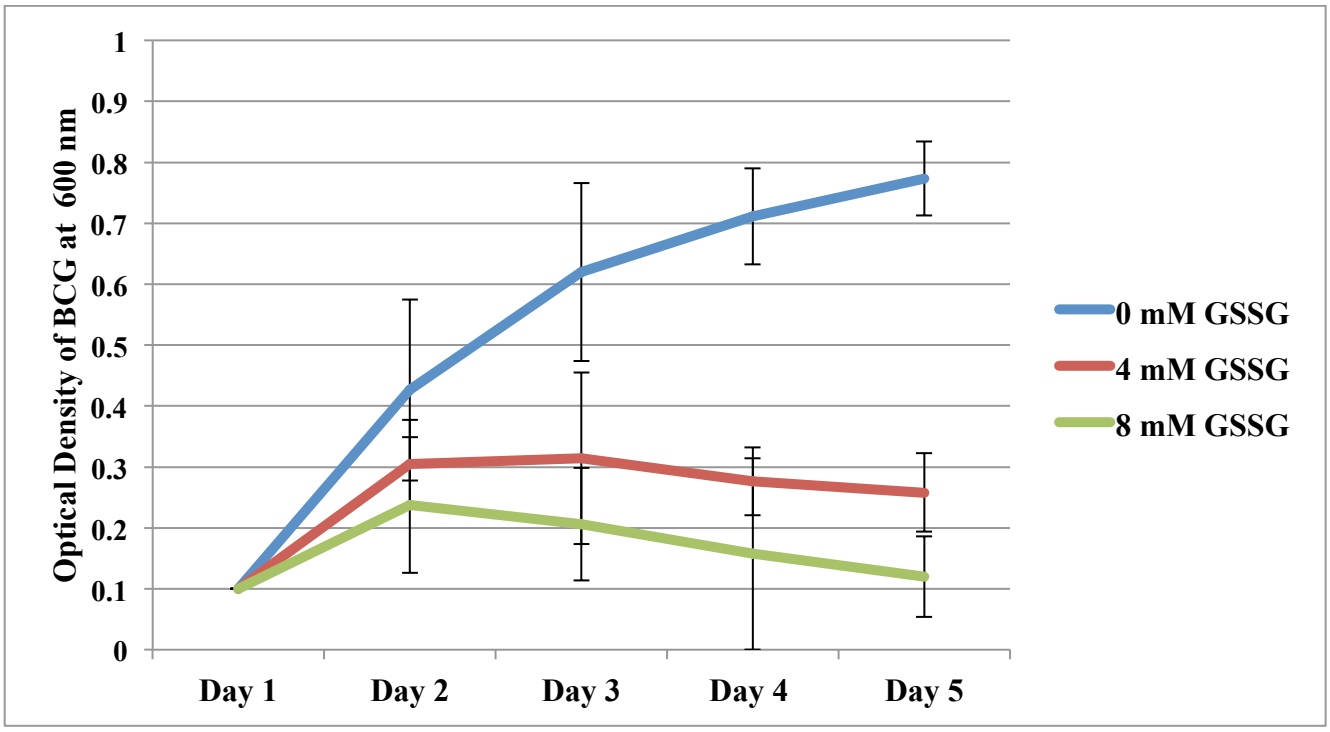

Figure 5a. Growth Curve of Mid-log BCG exposed to GSSG.

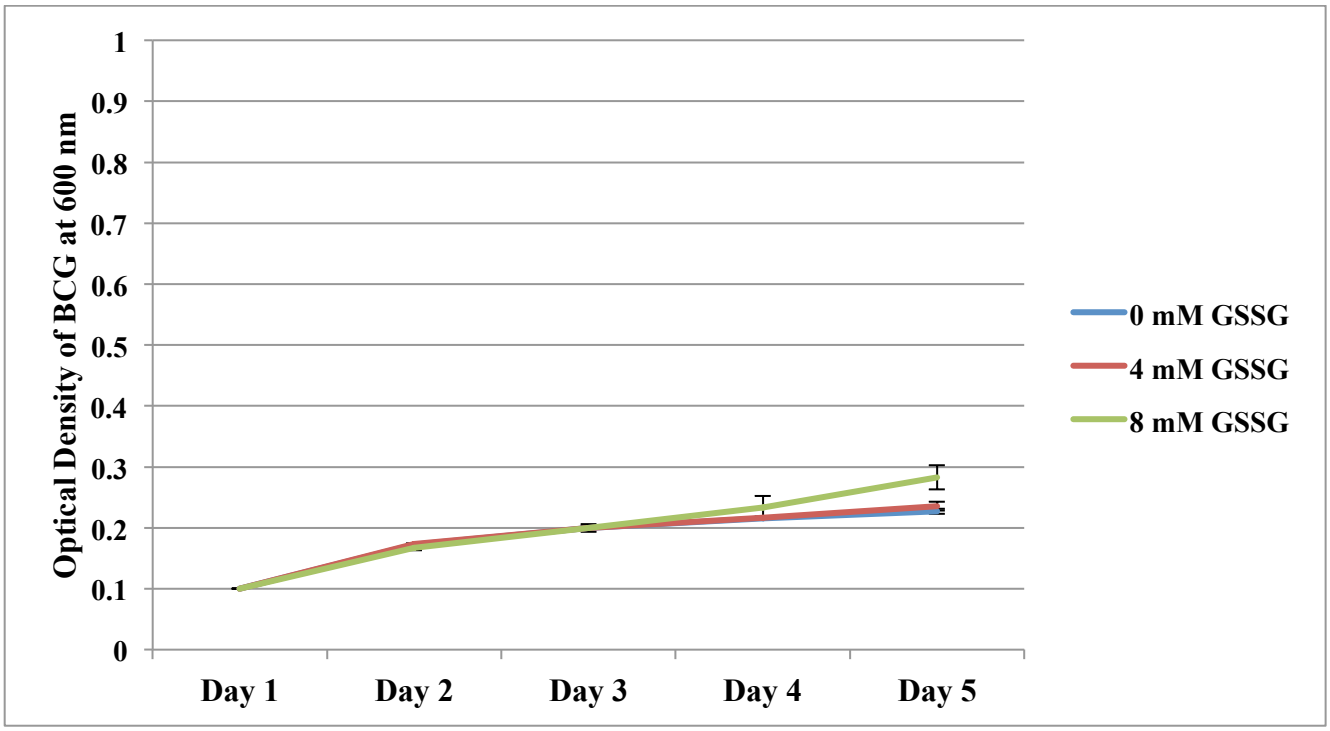

Figure 5b. Growth Curve of NRP BCG exposed to GSSG.

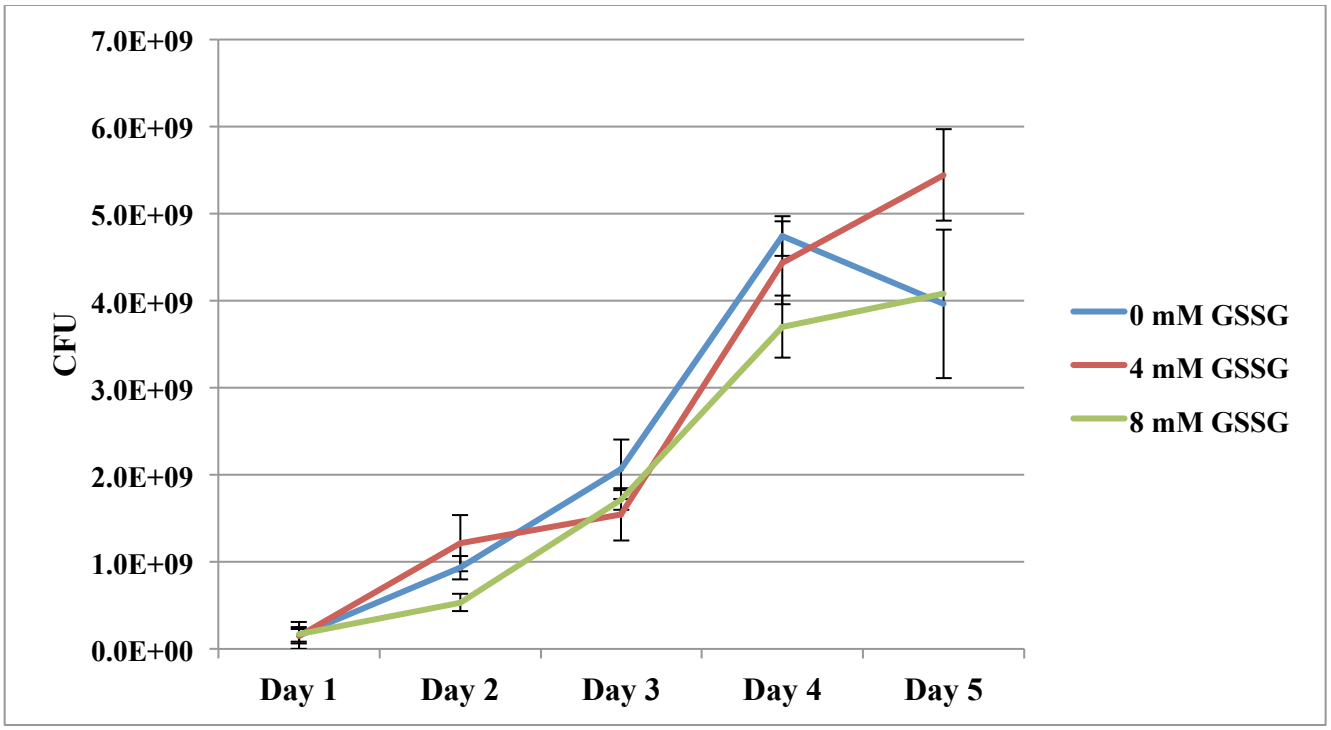

Figure 6a. Total Bacterial Cell Count of Mid-log BCG Exposed to GSSG.

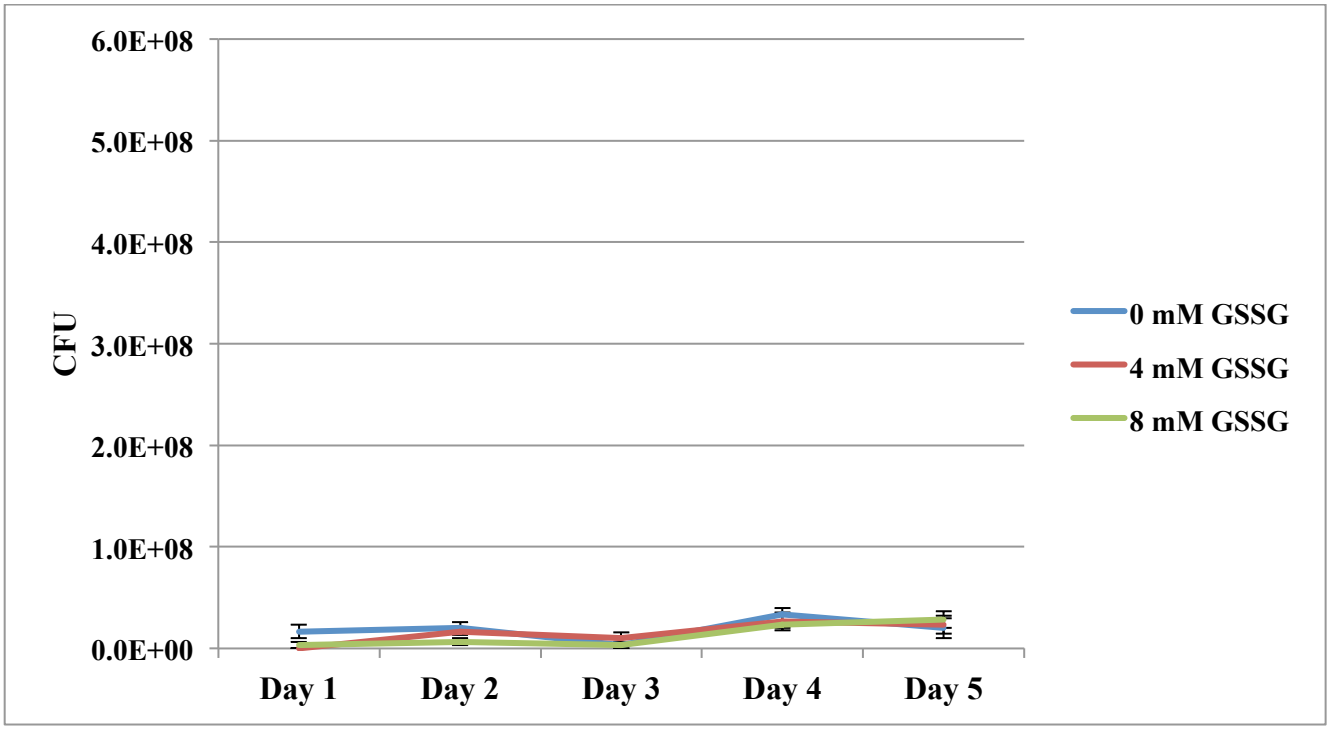

Figure 6b. Total Bacterial Cell Count of NRP BCG Exposed to GSSG.

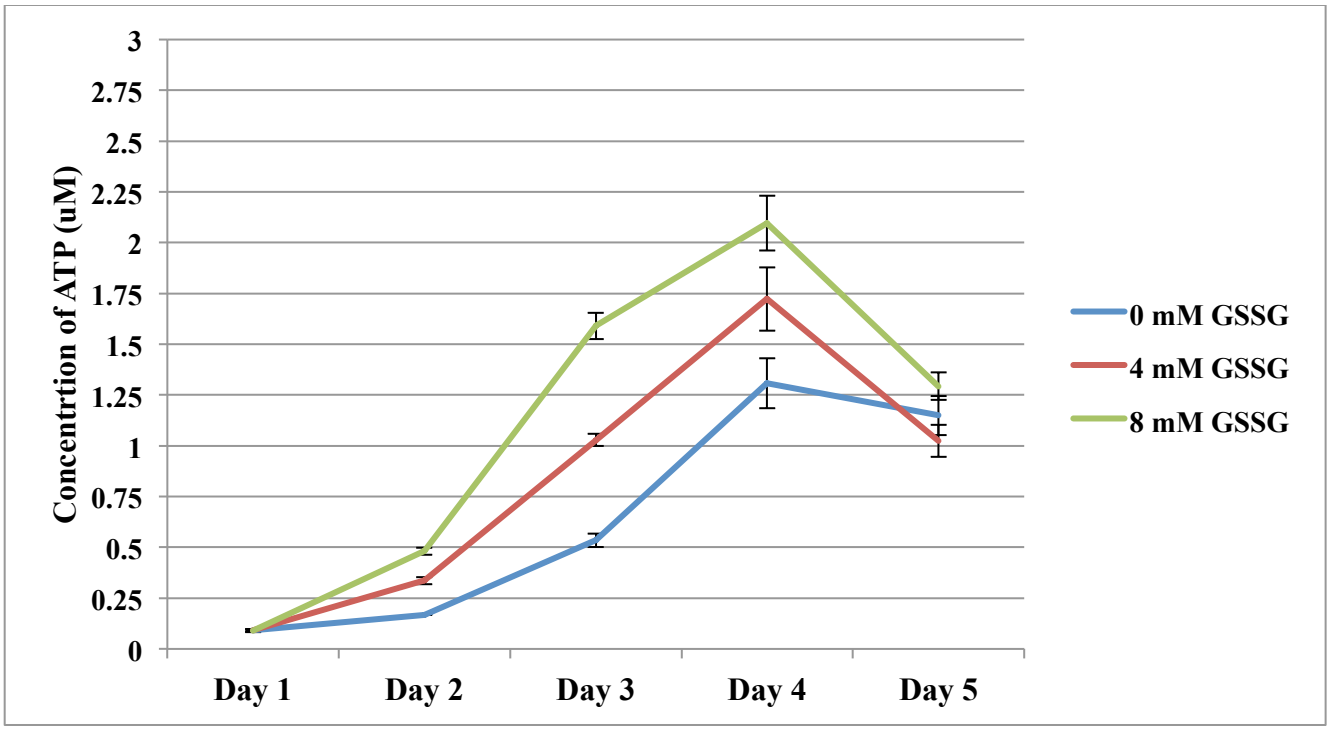

Figure 7a. Total Concentration of Free Intracellular ATP In Mid-log BCG Exposed to GSH.

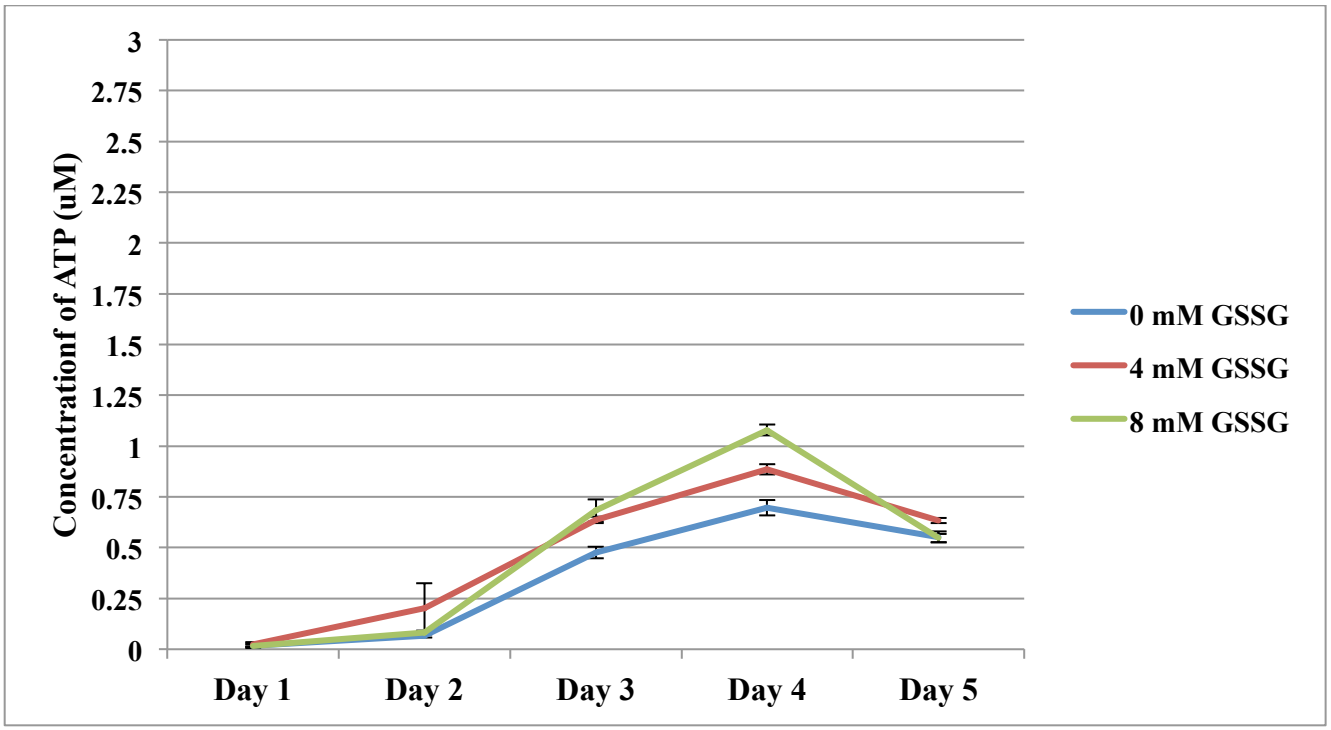

Figure 7b. Total Concentration of Free Intracellular ATP In NRP BCG Exposed to GSH.